

## Systematic study of low-spin states in even Cd nuclei

J. Kumpulainen, R. Julin, J. Kantele, A. Passoja,\* W. H. Trzaska, E. Verho, and  
J. Väärämäki

*Department of Physics, University of Jyväskylä, SF-40100 Jyväskylä, Finland*

D. Cutoiu and M. Ivascu

*Department of Heavy Ion Physics, Institute of Atomic Physics, Bucharest, R-76900, Romania*

(Received 15 January 1991)

Low-lying low-spin collective states in even  $^{106-112}\text{Cd}$  and  $^{116}\text{Cd}$  were investigated using in-beam and off-beam  $\gamma$ -ray and conversion-electron spectroscopy. New spin assignments and decay branching ratios for the levels in  $^{106}\text{Cd}$ ,  $^{108}\text{Cd}$ ,  $^{110}\text{Cd}$ , and  $^{112}\text{Cd}$  were obtained. The present results essentially complement the level systematics from  $^{106}\text{Cd}$  to  $^{120}\text{Cd}$ . From the new data, it is inferred that two sets of low-lying  $0^+$  states having different excitation characteristics cross between  $^{114}\text{Cd}$  and  $^{116}\text{Cd}$ . No corresponding crossing occurs on the neutron deficient side. New evidence for the existence of the proton-intruder states has been found.

PACS number(s): 21.10.Re, 23.20.-g, 25.40.-h, 27.60.+j

### I. INTRODUCTION

In the nuclei  $^{112}\text{Cd}$  and  $^{114}\text{Cd}$ , the quintuplet of levels at the excitation energy of the two-quadrupole-phonon states has given rise to many detailed theoretical and experimental investigations. It is generally believed that intruder configurations involving two-proton main shell excitations are present in odd-mass In and Sb nuclei and also in even-mass Sn nuclei [1]. These excitations provide an explanation for the observed rotational-like bands at low energies [2-4]. Strong population of low-lying  $0^+$  states of even Sn and Cd nuclei in the  $(^3\text{He}, n)$  two-proton transfer reaction [5] is regarded as a clear evidence of an intruding two-proton component of these states. A rotational band built on top of the first excited  $0^+$  state has been observed in  $^{110}\text{Cd}$  [6,7]. Moreover, fast  $E0$  transitions between excited  $0^+$  states in even Sn isotopes [8,9] indicate a sizable deformation associated with intruder  $0^+$  states.

Latest descriptions of collective properties of even-mass Cd isotopes have been based on the idea of mixing of intruder and vibrational phonon states [10-15]. In this way it has been possible to reproduce quite well most of the observed  $E2$  and  $E0$  transition rates between the relevant states in  $^{110}\text{Cd}$  [10],  $^{112}\text{Cd}$ , and  $^{114}\text{Cd}$  [11] as well as  $(t, p)$  transfer intensities to the  $0^+$  states in  $^{112}\text{Cd}$ ,  $^{114}\text{Cd}$ , and  $^{116}\text{Cd}$  [13]. The  $^{118}\text{Cd}$  and  $^{120}\text{Cd}$  isotopes have been studied in the view of mixing in Refs. [12,14,15]. Recently, Mach *et al.* [16] have measured lifetimes of the low-lying levels in the even  $^{116}\text{Cd}$ ,  $^{118}\text{Cd}$ , and  $^{120}\text{Cd}$ .

Fahlander *et al.* [17] have extensively studied  $^{114}\text{Cd}$  via

Coulomb excitation. They conclude that the vibrational model provides an overall better description of the data than the models mixing the vibrational and intruder states.

No consistent picture has emerged from the numerous theoretical interpretations of the available data. Different kinds of mixing have been introduced in the various studies, and even different states have been assigned as the intruders.

In locating intruder states, for example, in the Pt-Pb region, studies of level systematics have been of crucial importance. For the even-mass Cd isotopes, attempts to establish the systematics of the suggested intruder states have failed mainly because of the scarce experimental information, especially on the neutron deficient isotopes (see, e.g., Fig. 1 in Ref. [12] and Fig. 5 in Ref. [18]).

In the present work, a comprehensive experimental study of low-lying levels in  $^{106}\text{Cd}$ ,  $^{108}\text{Cd}$ ,  $^{110}\text{Cd}$ , and  $^{112}\text{Cd}$ , and a few complementary experiments on  $^{116}\text{Cd}$  were carried out using various in-beam and off-beam  $\gamma$ -ray and conversion-electron spectroscopy methods. The main emphasis in this work has been put on the systematic behavior of the  $(0_2^+, 2_2^+, 4_1^+, 0_3^+, 2_2^+)$  quintuplet of states. Inelastic proton scattering,  $(p, 2n)$  and  $(\alpha, 2n)$  reactions, as well as electron capture (EC)/ $\beta^+$ -decay of odd-odd In isomers, were found particularly advantageous in the population of low-lying nonyrast levels in Cd nuclei. This paper describes the experiments in detail; the resulting systematics has been shortly presented in Ref. [19].

As a result, new spin and level assignments as well as branching ratios obtained in this work render it possible to relate low-lying levels of similar character in even  $^{106-120}\text{Cd}$ . For the first time, the systematic behavior of the aforementioned quintuplet of states can be followed from  $^{106}\text{Cd}$  to  $^{120}\text{Cd}$ . The new data for  $^{112}\text{Cd}$  reveal a candidate for the intruder band, enabling us to look at the intruder band systematics up to spin  $6^+$  in the even  $^{110,112,114}\text{Cd}$  isotopes.

\*Present address: Department of Physics, University of Joensuu, SF-80101 Joensuu, Finland.

## II. EXPERIMENTAL METHODS

Inelastic scattering of protons was chosen as a tool for investigating all the stable even-mass Cd isotopes from  $^{106}\text{Cd}$  to  $^{116}\text{Cd}$  (except  $^{114}\text{Cd}$ ) in the present work. Although inelastic proton scattering has been applied to Cd isotopes, detailed conversion-electron and  $\gamma$ -ray spectroscopy studies have not been performed before this work [20–24]. The light stable Cd isotopes,  $^{106}\text{Cd}$  and  $^{108}\text{Cd}$ , we studied using for the first time the  $(p, 2n)$  reaction on the  $^{107}\text{Ag}$  and  $^{109}\text{Ag}$  target nuclei.

So far extensive gamma-ray spectroscopy following the  $\text{EC}/\beta^+$  decay of the odd-odd In isotopes has been carried out for Cd isotopes [20–23], while the electron spectroscopy only for  $^{106}\text{Cd}$  and  $^{108}\text{Cd}$  [18]. Recently, during the course of this work an  $E0$  study of  $^{110}\text{Cd}$  has been reported [25]. We used the  $(p, n)$  reaction to produce the odd-odd  $^{106,108,110}\text{In}$  isotopes and measured  $\gamma$ -ray and electron spectra following the  $\text{EC}/\beta^+$  decay of  $^{106,108,110}\text{In}$  isomers.

The existence of the stable Pd isotopes enable the  $(^3\text{He}, xn)$  and  $(\alpha, xn)$  reactions to be utilized in the study of the Cd isotopes. However, those reactions already preferably populate yrast states. The  $(\alpha, 2n)$  reaction has previously been used mainly in the study of the high-spin yrast states of the even  $^{106,108,112}\text{Cd}$  isotopes [26–28]. Recently, a comprehensive study of  $^{110}\text{Cd}$  has been published [7]. In the present work the  $(\alpha, 2n)$  reaction was performed for  $^{110}\text{Cd}$  and  $^{112}\text{Cd}$  to verify the results of Refs. [7,10,28].

A summary list of the experiments carried out in the present study of low-lying levels in even-mass Cd isotopes is presented in Table I.

### A. Inelastic proton scattering

An efficient method in locating levels and obtaining branching ratios was the detection of  $\gamma$  rays and conversion electrons from inelastic proton scattering at low bombarding energies. Due to the relatively high  $(p, n)$ -

reaction threshold, this method was especially useful for the  $^{106}\text{Cd}$  and  $^{108}\text{Cd}$  isotopes.

Gamma rays were measured in coincidence with scattered protons. The coincidence arrangement consisted of a 19% Ge detector positioned at about 3 cm from the target at  $90^\circ$  to the beam direction and three  $200\text{ mm}^2 \times 3\text{ mm}$  Si(Li) particle detectors which were positioned at about 2.5 cm from the target at angles of about  $140^\circ$  with respect to the beam. Targets were 1–2  $\text{mg}/\text{cm}^2$  thick metallic foils of enriched  $^{106}\text{Cd}$  (90%),  $^{108}\text{Cd}$  (74%),  $^{110}\text{Cd}$  (96%),  $^{112}\text{Cd}$  (96%), and  $^{116}\text{Cd}$  (94%). Beam energies of  $E_p = 7\text{--}9\text{ MeV}$  were used. The energy resolution in the summed Si(Li) spectra was about 200 keV, which allowed a sufficient level selection. The arrangement tends to moderate proton-gamma angular-correlation effects, which we concede to cause about 10% minimum uncertainty to the  $\gamma$ -ray intensities. In Figs. 1(b) and 1(c) typical proton-gated  $\gamma$ -ray spectra corresponding to 0.2–0.3 MeV wide proton gates are illustrated.

It was often useful to examine  $\gamma$ -ray gated proton spectra (Fig. 2). From these spectra  $\gamma$ -ray placements and branching ratios were confirmed and, moreover, the  $\gamma$ -ray population of a state from higher-lying levels could be observed directly.

Our combination electron spectrometer system [29] including a Siegbahn-Slätis type of magnetic lens and a cooled  $110\text{ mm}^2 \times 3\text{ mm}$  Si(Li) detector was employed in the conversion-electron measurements. For suppressing the delayed  $\beta^-$  background, a narrow time gate, synchronized with the cyclotron beam micropulse (rf) was used. Useful electron spectra from the inelastic proton scattering were obtained for the  $^{106}\text{Cd}$  [Fig. 1(d)],  $^{108}\text{Cd}$ , and  $^{110}\text{Cd}$  isotopes.

### B. $(p, 2n)$ reaction

To further study low-spin properties of the  $^{106}\text{Cd}$  and  $^{108}\text{Cd}$  isotopes, we employed the  $(p, 2n\gamma)$  reaction. The targets were enriched self-supporting 9.3  $\text{mg}/\text{cm}^2$  thick  $^{107}\text{Ag}$  (98%) and 7.6  $\text{mg}/\text{cm}^2$  thick  $^{109}\text{Ag}$  (99%) foils.

TABLE I. List of the experiments for even-mass  $^{106\text{--}112,116}\text{Cd}$  in the present work.

Reaction	Type of spectroscopy <sup>a</sup>	Mass number of Cd isotope investigated
$(p, p')$	$e^-, \gamma$	106, 108, 110
	$p\gamma$ coin	106, 108, 110, 112, 116
$(p, 2n)$	$\gamma$	106, 108
	$\gamma\gamma$ coin <sup>b</sup>	106, 108
	$\gamma(\theta)$	106, 108
	$\gamma(E_p)$	106, 108
$(\alpha, 2n)$	$\gamma$	110, 112
	$\gamma\gamma$ coin	110, 112
	$\gamma(\theta)$	110, 112
	$\gamma(E_\alpha)$	110, 112
In decay	$e^-, \gamma$	106, 108, 110

<sup>a</sup> $e^-$  indicates electron spectroscopy, singles mode;  $\gamma$  indicates  $\gamma$ -ray spectroscopy, singles mode;  $\gamma(\theta)$  and  $\gamma(E)$  mean  $\gamma$ -ray angular-distribution and excitation-function measurements, respectively.

<sup>b</sup>Compton-suppressed  $\gamma\gamma$  coincidences.

Gamma-gamma coincidences were measured at  $E_p = 14.5$  MeV and at  $E_p = 12.7$  MeV for  $^{106}\text{Cd}$  and  $^{108}\text{Cd}$ , respectively. The coincidence arrangement consisted of two Compton-suppressed Ge detectors (20–25%) of the NORDBALL type in a close measurement geometry, designed for low-multiplicity experiments. About  $3.3 \times 10^6$  and  $1.4 \times 10^6$  Compton-suppressed coincidence events were recorded in these measurements for  $^{106}\text{Cd}$  and  $^{108}\text{Cd}$ , respectively. In Fig. 3, a spectrum corresponding to a gate on  $\gamma$  rays of the  $2_1^+ - 0_1^+$  transition in  $^{108}\text{Cd}$  is illustrated.

For the spin and multipolarity determination, angular-distribution measurements for  $\gamma$  rays from the  $^{107}\text{Ag}(p, 2n)^{106}\text{Cd}$  ( $E_p = 14.5$  MeV) and  $^{109}\text{Ag}(p, 2n)^{108}\text{Cd}$  ( $E_p = 12.7$  MeV) reactions were carried out at five angles between  $90^\circ$  and  $158^\circ$ .

Especially useful in assigning spins of levels in  $^{106}\text{Cd}$  and  $^{108}\text{Cd}$  were the  $\gamma$ -ray excitation-function measurements in the  $(p, 2n)$  reactions between  $E_p = 12.3$  and 17.4 MeV. Typical resulting curves are shown in Figs. 4 and 5.

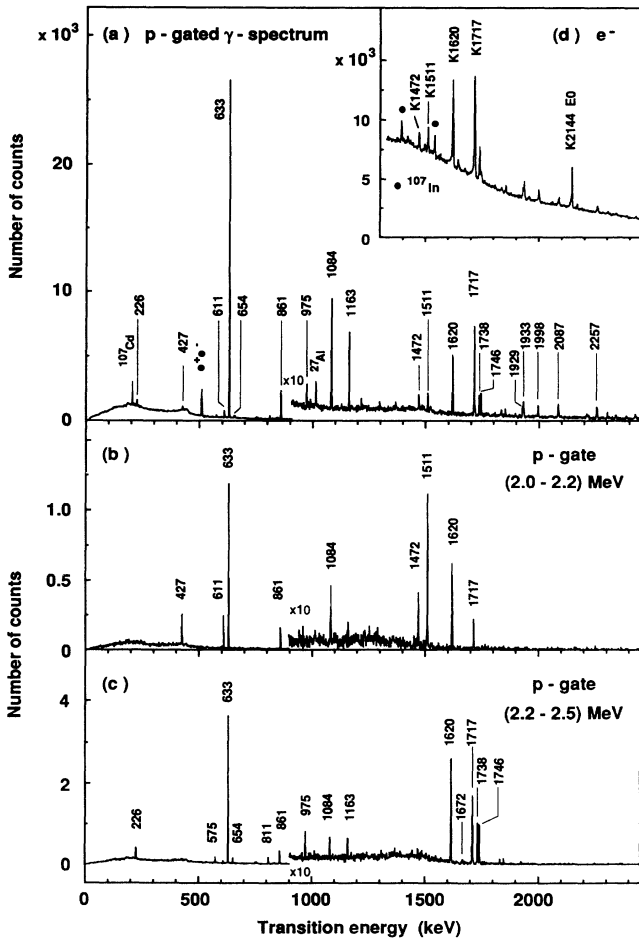


FIG. 1. Proton gated  $\gamma$ -ray spectra (a)–(c) and singles conversion-electron spectrum (d) from the  $^{106}\text{Cd}(p, p')$  reaction at  $E_p = 7.5$  MeV. Proton gates indicated in the figure correspond to the excitation energies in  $^{106}\text{Cd}$ .

### C. $(\alpha, 2n)$ reaction

For the study of low-lying levels of the  $^{110}\text{Cd}$  and  $^{112}\text{Cd}$  isotopes, the  $(\alpha, 2n\gamma)$  reaction on enriched  $^{108}\text{Pd}$  and  $^{110}\text{Pd}$  targets was also used. The  $\gamma\gamma$ -coincidence, angular-distribution, and excitation-function measurements were performed.

About  $18 \times 10^6$   $\gamma\gamma$  coincidences were recorded for  $^{110}\text{Cd}$  at  $E_\alpha = 18$  MeV by employing 20% and 25% Ge detectors in the conventional close-measurement geometry without anti-Compton shields. In the  $\gamma\gamma$ -coincidence measurement for  $^{112}\text{Cd}$  at  $E_\alpha = 20$  MeV, three Ge detectors (40%, 25%, and 15%) were used in close geometry and about  $60 \times 10^6$   $\gamma\gamma$  coincidences were recorded.

In the  $\gamma$ -ray excitation-function measurements  $\alpha$ -beam energies from 17.0 to 20.0 MeV were used (Figs. 6 and 7). In the angular-distribution measurement,  $\gamma$ -ray spectra at five angles between  $90^\circ$  and  $155^\circ$  were measured at  $E_\alpha = 18$  MeV and  $E_\alpha = 20$  MeV for  $^{110}\text{Cd}$  and  $^{112}\text{Cd}$ , respectively.

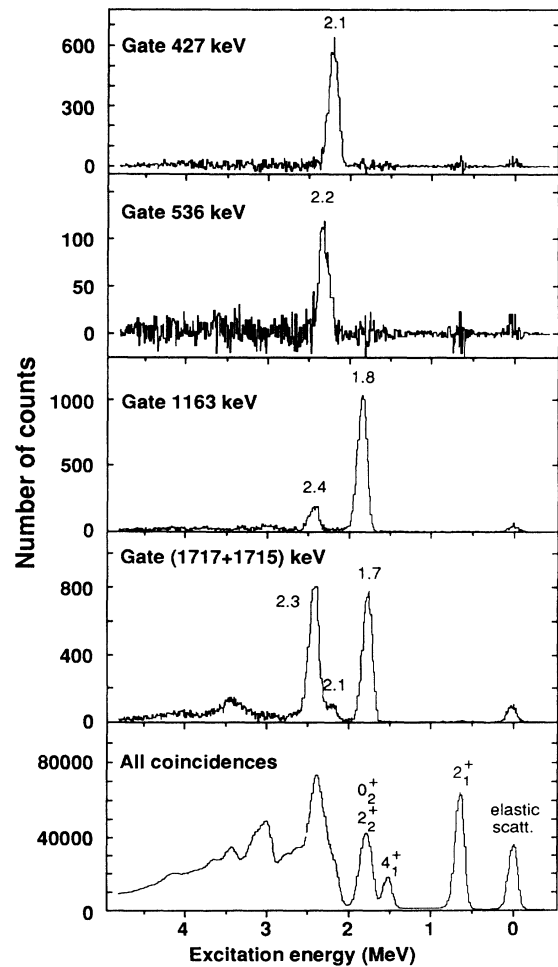


FIG. 2. Gamma-ray gated proton spectra from the  $^{106}\text{Cd}(p, p')$  reaction. Spectra of protons in coincidence with the indicated  $\gamma$  rays are shown. The events in the peak denoted as “elastic scatt.” originate from random coincidences.

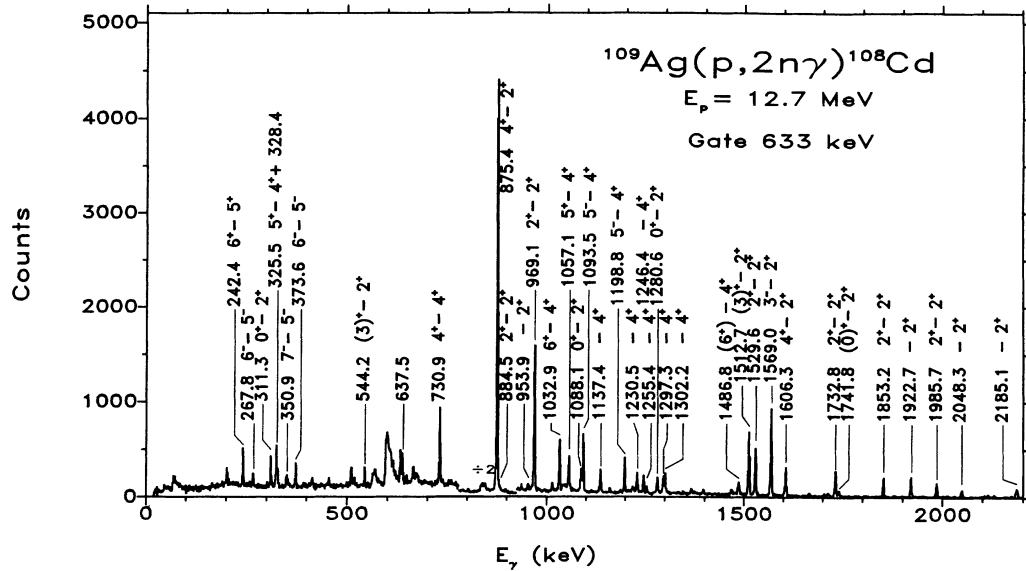


FIG. 3. Gamma-rays in coincidence with the  $2_1^+ - 0_1^+$  transition in  $^{108}\text{Cd}$  from the reaction  $^{109}\text{Ag}(p,2n)$  at  $E_p = 12.7$  MeV. Two NORDBALL-type Compton-suppression spectrometers have been used.

#### D. Decay measurements

In addition to the in-beam experiments, valuable information for  $^{106}\text{Cd}$ ,  $^{108}\text{Cd}$ , and  $^{110}\text{Cd}$  was obtained in off-beam measurements of  $\gamma$ -ray and conversion-electron spectra following the  $\text{EC}/\beta^+$  decay of odd-odd In iso-

mers. The decaying isomers were the  $(2^+)$  (5.3 min) and  $7^+$  (6.3 min) states in  $^{106}\text{In}$ , the  $2^+$  (39.6 min) and  $7^+$  (58.0 min) states in  $^{108}\text{In}$ , and the  $2^+$  (69 min) and  $7^+$  (4.9 h) states in  $^{110}\text{In}$ . They were produced in bombardments of enriched  $^{106}\text{Cd}$ ,  $^{108}\text{Cd}$ , and  $^{110}\text{Cd}$  foils by the 10–12.5 MeV protons. In the  $\gamma$ -ray measurements multispectra were recorded. In the conversion-electron measurements the aforementioned magnetic lens plus Si(Li) electron spectrometer was employed. In Fig. 8 a part of a  $\gamma$ -ray and a conversion-electron spectrum from the  $\text{EC}/\beta^+$  decay of  $^{108}\text{In}$  are presented.

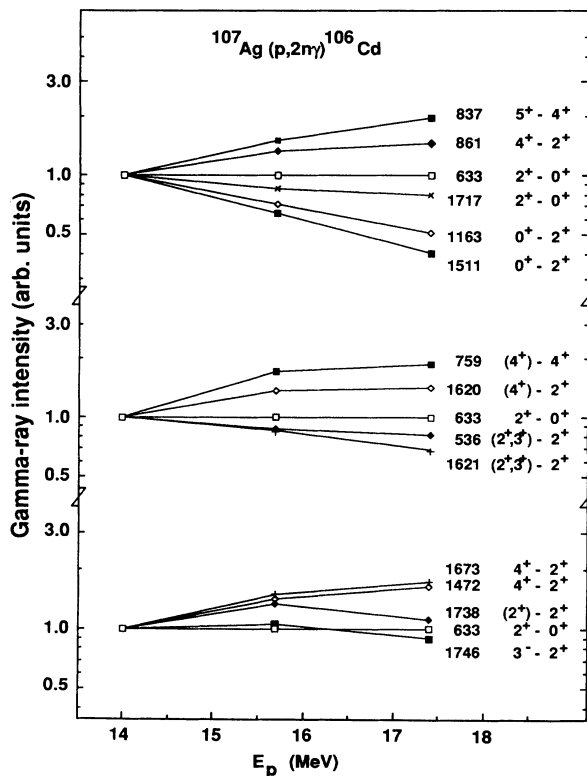


FIG. 4. Excitation functions for some  $\gamma$  rays from the  $^{107}\text{Ag}(p,2n)^{106}\text{Cd}$  reaction. The relative yields normalized at  $E_p = 14$  MeV are plotted.

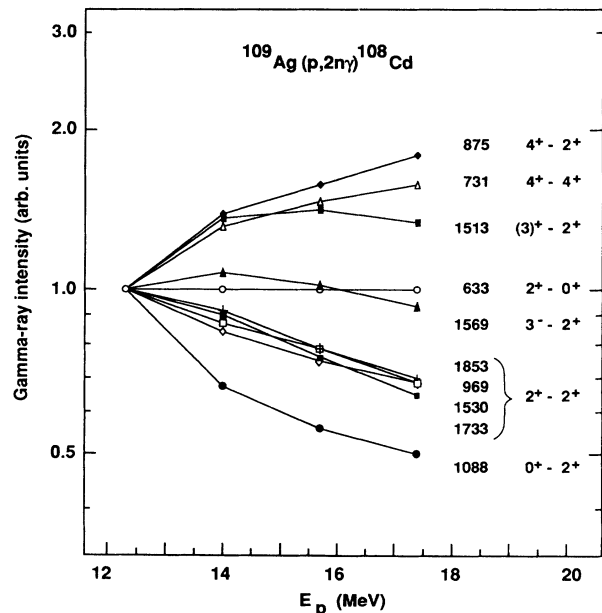


FIG. 5. Excitation functions for some  $\gamma$  rays from the  $^{109}\text{Ag}(p,2n)^{108}\text{Cd}$  reaction. The relative yields normalized at  $E_p = 12.3$  MeV are plotted.

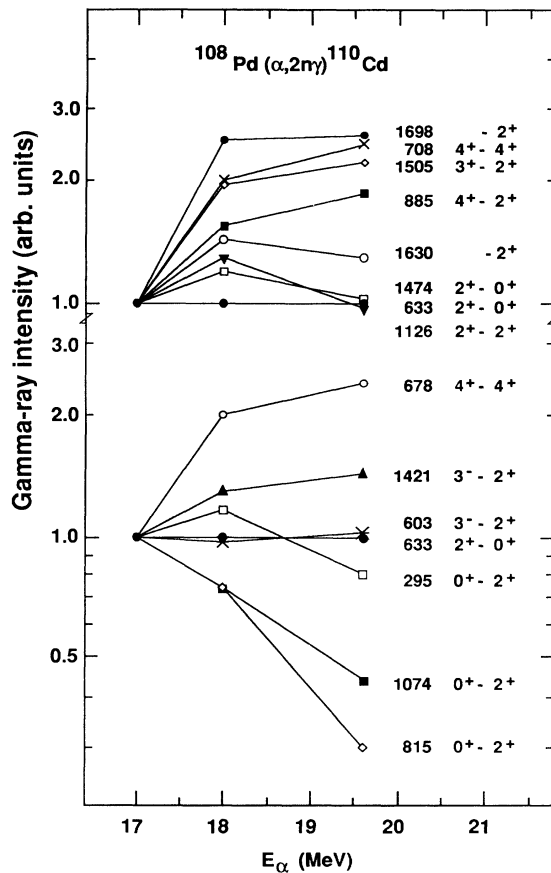


FIG. 6. Excitation functions for some  $\gamma$  rays from the  $^{108}\text{Pd}(\alpha,2n)^{110}\text{Cd}$  reaction. The relative yields normalized at  $E_\alpha = 17$  MeV are plotted.

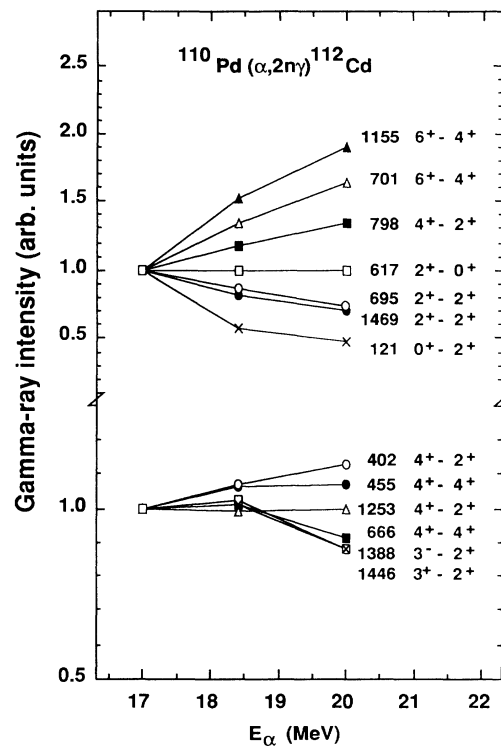


FIG. 7. Excitation functions for some  $\gamma$  rays from the  $^{110}\text{Pd}(\alpha,2n)^{112}\text{Cd}$  reaction. The relative yields normalized at  $E_\alpha = 17$  MeV are plotted.

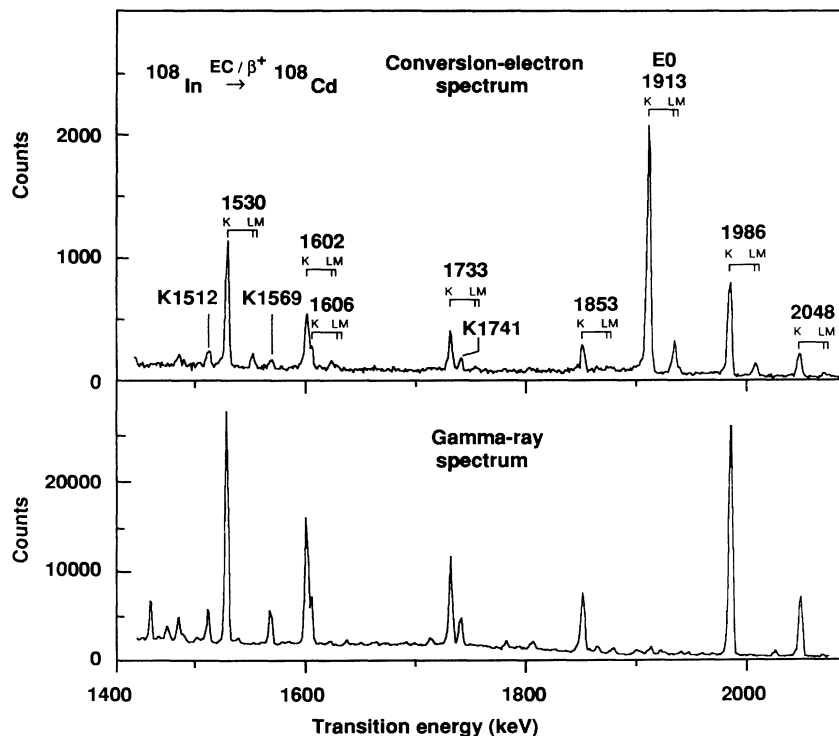


FIG. 8. The singles  $\gamma$ -ray (bottom) and conversion-electron (top) spectra following the  $\text{EC}/\beta^+$  decay of  $^{108}\text{In}$ . The electron spectrum is shifted so that the  $K$  conversion-electron peaks coincide with the corresponding  $\gamma$  rays.

### III. EXPERIMENTAL RESULTS

A summary of the results is given in Tables II-VI for each isotope. As only the low-lying collective states were of interest we limited level-energy range to that below about 2.5 MeV for  $^{106}\text{Cd}$ ,  $^{108}\text{Cd}$ , and  $^{110}\text{Cd}$  and below 2 MeV for  $^{112}\text{Cd}$  and  $^{116}\text{Cd}$ . Above that energy the noncollective two quasiparticle excitations become more important. The  $\gamma$ -ray intensities from different reactions applied in this work are given in the tables. One should note that the  $\gamma$ -ray intensities obtained from the  $(p,p')$  reaction correspond to the direct level population and are thus related to the  $(p,p')$  cross section, since they do not

include  $\gamma$ -ray feeding. However, the  $\gamma$ -ray branching ratios from each level can be compared in different reactions. The internal  $K$ -conversion coefficients presented in the tables are from the present decay studies of odd-odd In and from the  $(p,p')$  measurements. The angular-distribution coefficients  $A_{22}$  and  $A_{44}$  are from the  $(p,2n)$  reaction for  $^{106,108}\text{Cd}$  and from the  $(\alpha,2n)$  reaction for  $^{110}\text{Cd}$  and  $^{112}\text{Cd}$ . The excitation-function curves shown in Figs. 4 ( $^{104}\text{Cd}$ ), 5 ( $^{108}\text{Cd}$ ), and 6 ( $^{110}\text{Cd}$ ) illustrate at least one transition from each level, when possible. Only curves relevant for the discussion on  $^{112}\text{Cd}$  are shown in Fig. 7.

The level schemes of the even-mass Cd isotopes ob-

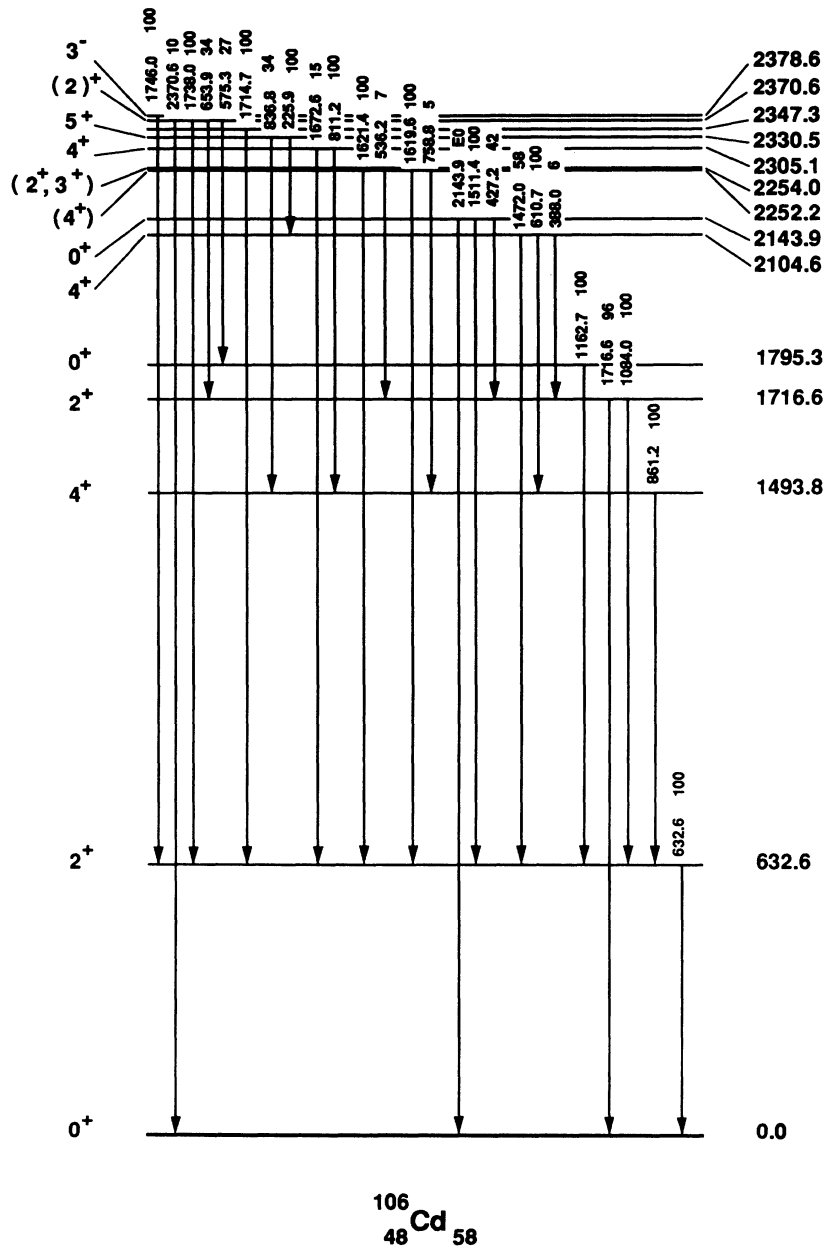


FIG. 9. The level scheme of  $^{106}\text{Cd}$  as obtained in this work. The relative  $\gamma$ -ray intensities of the depopulating transitions are marked for each level.

tained in this work are presented in Figs. 9 ( $^{106}\text{Cd}$ ), 10 ( $^{108}\text{Cd}$ ), 11 ( $^{110}\text{Cd}$ ), 12 ( $^{112}\text{Cd}$ ), and 13 ( $^{116}\text{Cd}$ ). The placements of the transitions are based on the  $\gamma\gamma$ - and  $p\gamma$ -coincidence data. The adopted  $\gamma$ -ray branching ratios shown in the level schemes are obtained by averaging the values from different experiments. The spin and parity assignments are inferred from the excitation functions and the angular distributions of  $\gamma$  rays and from the conversion-electron data.

#### A. The nucleus $^{106}\text{Cd}$

The experiments presented in this work have revealed two new levels in the level scheme of  $^{106}\text{Cd}$  below the 2.4

MeV excitation, while no evidence was found for two levels reported earlier. Eight new transitions were observed and for six levels the  $I^\pi$  value is new or revised.

The earlier assignments [20] of  $4^+$  and  $2^+$  for the 1493.8 and 1716.6 keV levels are in agreement with the data given in Table II and the excitation-function data of Fig. 4. The present average value of 0.96(15) for the  $\gamma$ -ray branching ratio of the 1716.6 and 1084.0 keV transitions from the  $2^+$  (1716.6 keV) level is somewhat smaller than the value of 1.4(3) adopted in Ref. [20]. This may be due to the difficulties in the analysis of close-lying 1716.6 and 1714.7 keV lines.

The 1795.3 keV level has previously been populated in the beta decay of the low-spin isomer of  $^{106}\text{In}$  [18,30,31],

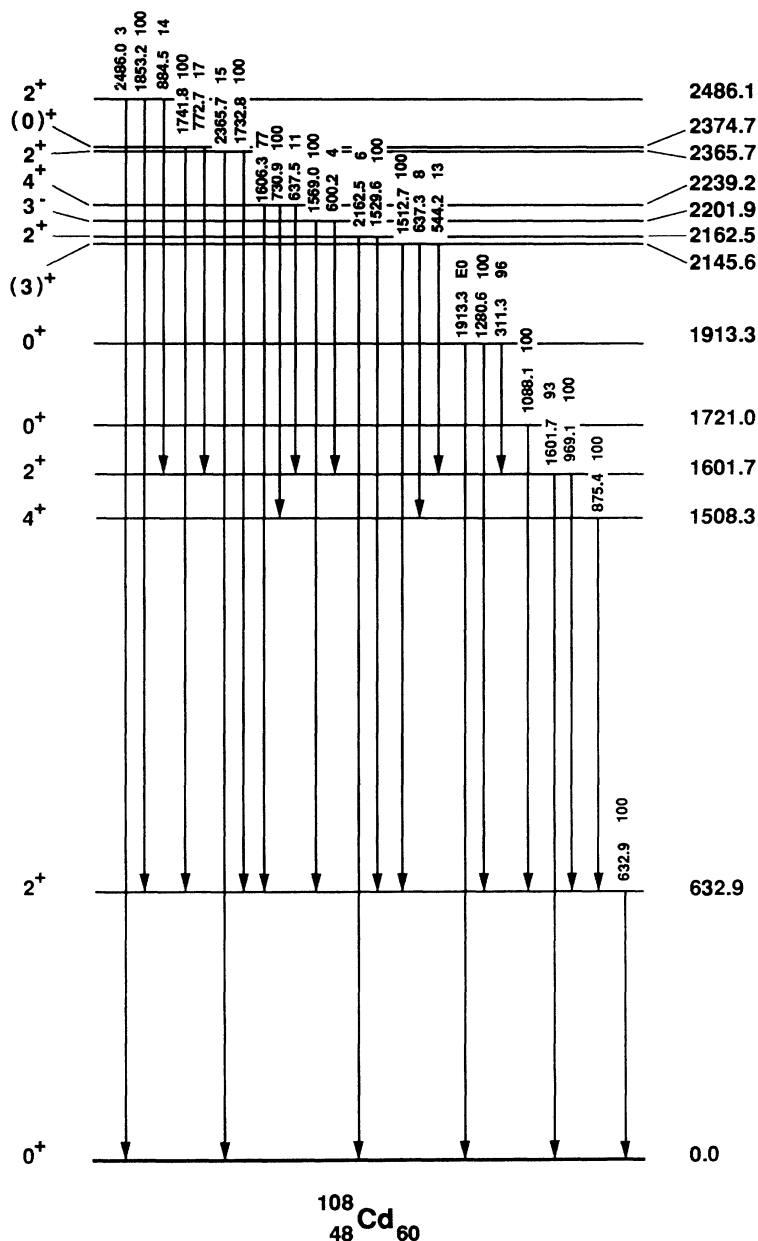


FIG. 10. The level scheme of  $^{108}\text{Cd}$  as obtained in this work. The relative  $\gamma$ -ray intensities of the depopulating transitions are marked for each level.

and in the inelastic scattering of alpha particles [32]. The spin and parity assignment of  $4^+$  for this state was proposed in Ref. [30]. However, the present angular distribution of the depopulating 1162.7 keV transition is nearly isotropic. Moreover, the excitation function of this transition has a clear  $I=0$  character (Fig. 4). Thus, this state can be identified with the first excited  $0^+$  state in  $^{106}\text{Cd}$ . In spite of the relatively strong population of this  $0^+$  state in the inelastic proton scattering no  $E0$  transition from this state to the ground state is observed in our conversion-electron measurements, which must be due to the fast competing 1162.7 keV  $E2$  transition deexciting this level. In the 1162.7 keV  $\gamma$ -ray gated proton spectrum of Fig. 2 one observes a peak at  $E_x=2.4$  MeV indi-

cating feeding of this level from a level at about 2.4 MeV (see the discussion for the 2370.6 keV level).

No evidence for the 2034.8 keV level reported in Refs. [33] and [18] is found in this work. The level has been tentatively assigned as  $I^\pi=0^+$  in Ref. [33], but was not confirmed in the later study of the same authors [18]. Figure 14 shows that the 1402.1 keV transition which was suggested to depopulate the 2034.8 keV level in fact is in coincidence with both of the 632.6 and 861.2 keV transitions, thus depopulating a level at higher excitation energy. The  $p\gamma$ -coincidence data confirm this result.

For the 2104.6 keV level we confirm  $I^\pi=4^+$  through the excitation functions, angular distributions, and conversion-electron coefficients of the depopulating

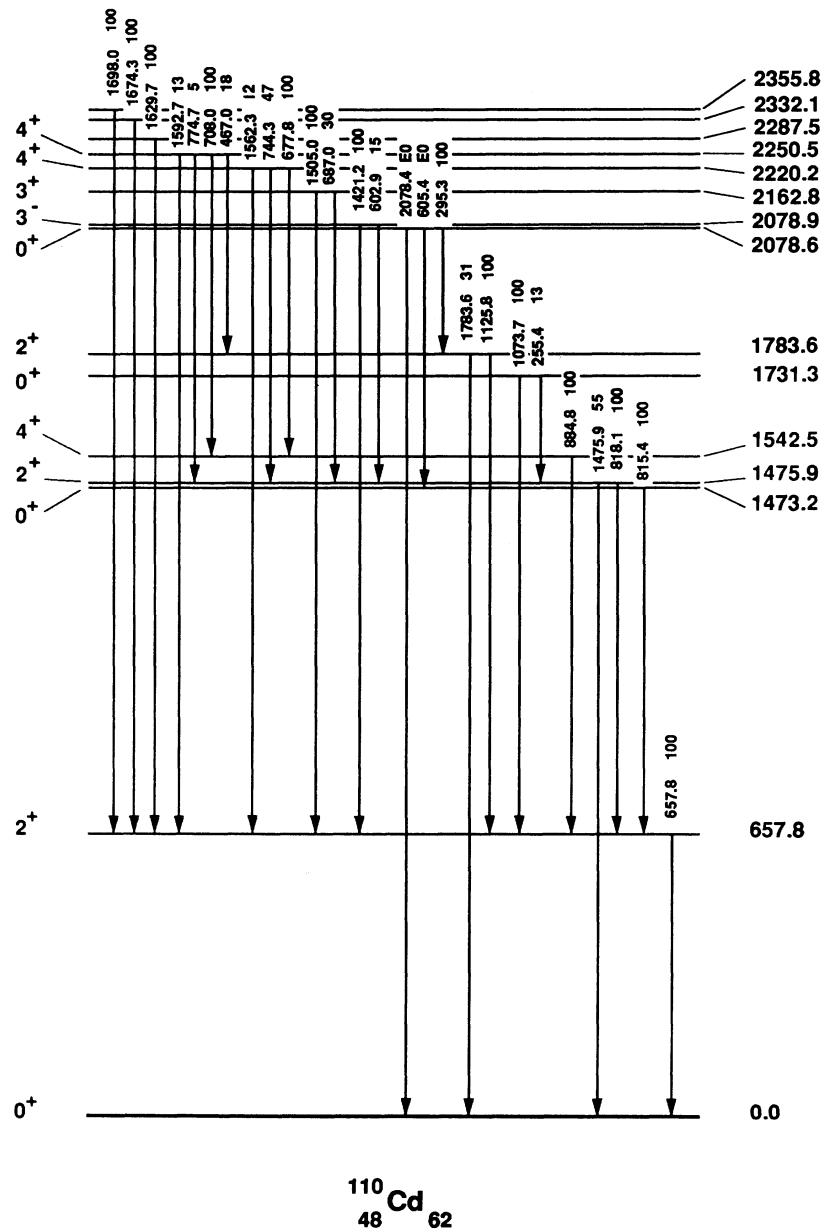


FIG. 11. The level scheme of  $^{110}\text{Cd}$  as obtained in this work. The relative  $\gamma$ -ray intensities of the depopulating transitions are marked for each level.



388.0, 610.7, and 1472.0 keV transitions. The  $\gamma$ -ray branchings of that level are in agreement with Ref. [20].

We identify a new level at 2143.9 keV for which we firmly assign  $I^\pi=0^+$ . From the conversion-electron and  $\gamma$ -ray spectra in the  $(p,p')$  reaction a new 2143.9 keV  $E0$  transition could be established [Fig. 1(d)]. In the  $p\gamma$ -coincidence experiments the corresponding new 1511.4 and 427.2 keV  $E2$  transitions to the  $2_1^+$  and  $2_2^+$  states [Fig. 1(b)] are observed, and the placement is confirmed by the  $\gamma\gamma$ -coincidence measurements. The slope of the 1511 keV  $\gamma$ -ray excitation-function curve in the  $(p,2n)$  reaction (Fig. 4) is typical for  $\gamma$  rays from a  $0^+$  level. The connecting  $E0$  transition between the  $0_3^+$  and  $0_2^+$  states is not observed in our electron spectra from the  $(p,p')$  reaction or from the  $^{106}\text{In}$  EC/ $\beta^+$  decay. The 427.2 keV  $\gamma$ -ray gated proton spectrum (Fig. 2) shows no feeding of this level from higher lying levels.

For the 2252.2(6) keV level we tentatively assigned  $I^\pi=(4^+)$ , mainly on the basis of the  $(p,2n)$  excitation

functions for the depopulating 758.8 keV (new) and 1619.6 keV  $\gamma$  transitions to the  $4_1^+$  and  $2_1^+$  states, respectively (Fig. 4). This level is probably the same as the 2252.7 keV  $(3,4^+)$  level seen in an earlier in-beam  $\gamma$ -ray study of the  $^{97}\text{Mo}(^{12}\text{C},3n)$  reaction [34], and the same as the 2252.9 keV level observed in the  $^{106}\text{In}$  decay study [18]. The present  $p\gamma$ - and  $\gamma\gamma$ -coincidence data show that this level is fed from the level at about 3020 keV (which is beyond the energy region considered here) by the 767 keV transition (see the gate on the 759 keV  $\gamma$  rays in Fig. 14).

The 2254.0(5) keV level has a low-spin value  $I^\pi=(2^+,3^+)$  according to the  $(p,2n)$  excitation functions for the depopulating 536.2 keV (new) and 1621.4 keV  $\gamma$  transitions (Fig. 4). There is no transition to the ground state from this state, which would favor the  $3^+$  assignment. Also the angular distribution of the 536.2 keV transition with the large negative  $A_{22}$  is consistent with the  $I^\pi=3^+$ . Roussiere *et al.* [18] have reported the

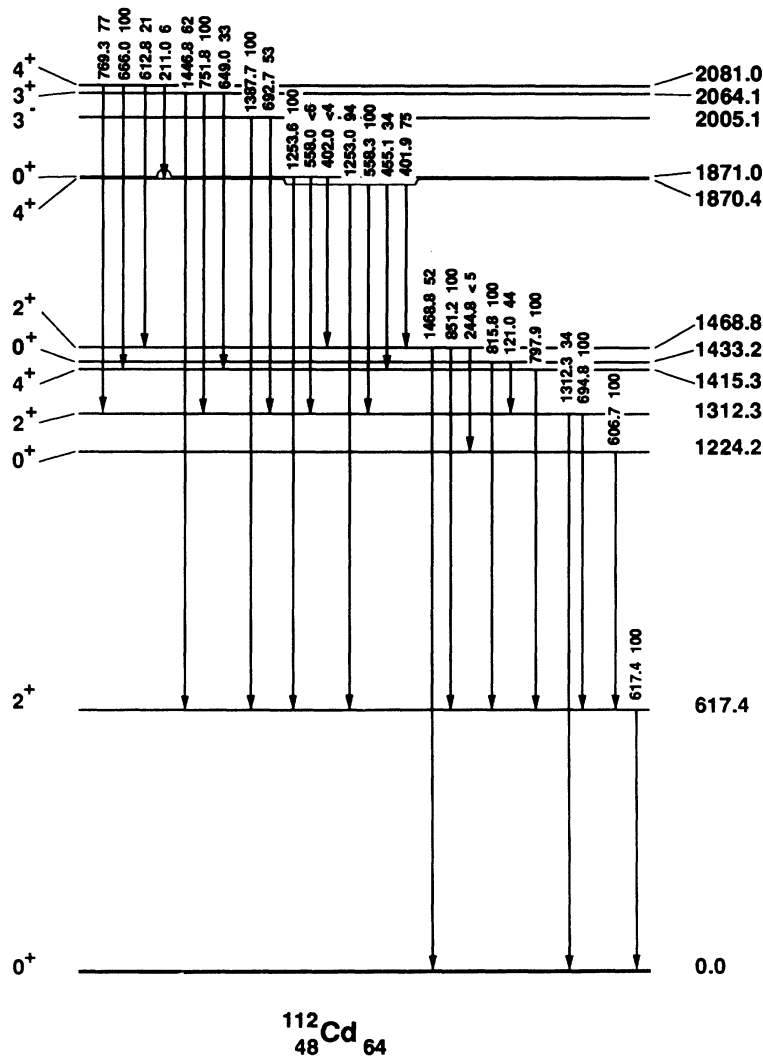


FIG. 12. The level scheme of  $^{112}\text{Cd}$  as obtained in this work. The relative  $\gamma$ -ray intensities of the depopulating transitions are marked for each level. Note that the  $E0$  transitions measured in Ref. [41] are not included in the figure.

1620.2 and 1622.1 keV transitions, of which the latter one was not placed into their level scheme, therefore supporting our result of two close-lying levels.

The 2305.1 keV level has earlier been assigned as  $I=(4)$  in the in-beam  $^{96,97}\text{Mo}(^{13,12}\text{C}, 3n)$  study [34]. The present excitation functions and the angular distributions of the 811.2 keV transition and of a new 1672.6 keV  $\gamma$  transition from this level (Fig. 4) are in accord with the old result. In addition, the conversion coefficients of both of these transitions (Table II) imply a positive parity for this state, thus revealing  $I^\pi=4^+$  for the state.

The present data for the 2330.5 keV level confirms the  $\gamma$ -ray branching ratio and  $I^\pi=5^+$  adopted for this level in Ref. [20].

In the level scheme we have omitted the 2338.7 keV level seen in the  $(^{12}\text{C}, 3n)$  and  $(^{13}\text{C}, 3n)$  reactions [34]. The 1704.5 keV transition, which was previously suggested to deexcite this level, is in our  $\gamma\gamma$ -coincidence measurements observed to feed the 1494 keV  $4_1^+$  level. This result is further confirmed by the  $p\gamma$  coincidences.

The 2347.8 keV level is strongly populated in the

present  $(p, p')$  experiment, but the  $(2)^+$  assignment of Ref. [20] could not be verified due to the complexity of the depopulating 1714.7 keV transition (close-lying 1716.6 keV transition).

The level at 2370.6 keV has been associated with an  $L=3$  state at 2366 keV observed in a  $(p, p')$  experiment [35] and thus suggested to be the first excited  $3^-$  state [26]. However, in addition to the 1738.0 keV transition to the  $2_1^+$  state and a new 653.9 keV transition to the  $2_2^+$  state, we observe a 575.3 keV transition to the newly assigned  $0_2^+$  state and a 2370.6 keV transition to the ground state (see the 1163 keV gate in Figs. 2 and 14). The measurement of the  $K$  internal conversion coefficients for these transitions is obscured by the  $L$ -conversion lines of the strong  $E2$  transitions (552, 633, and 1717 keV). However, the  $K$ -conversion coefficient for the 575.3 keV transition could be obtained in the  $(p, p')$  reaction where the 3044 keV  $(8)^+$  level decaying by the interfering 552.4 keV transition is not populated. The  $E2$  multipolarity of the 575.3 keV transition definitively rules out the  $3^-$  assignment. Consequently, a tentative  $(2^+)$  assignment for

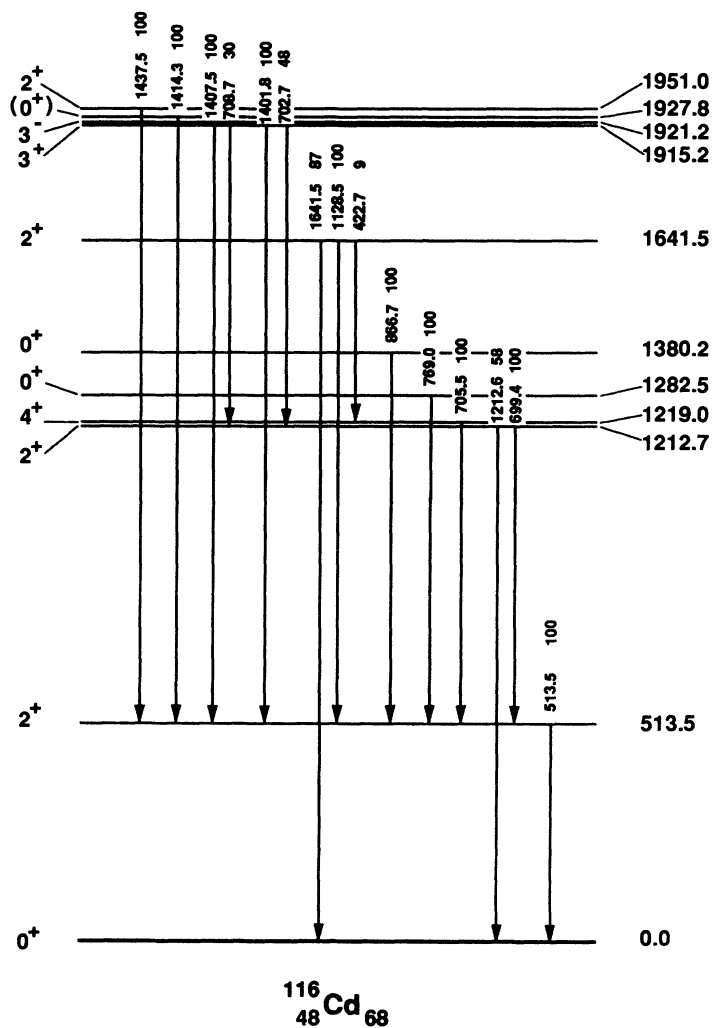


FIG. 13. The level scheme of  $^{116}\text{Cd}$  as obtained in this work. The relative  $\gamma$ -ray intensities of the depopulating transitions are marked for each level.

this state is suggested in this work.

The 2378.6 keV level is strongly populated in our  $(p, p')$  experiment. The level has been observed in Refs. [30] and [31], but no spin and parity assignments have been proposed. The conversion-coefficient limit definitely gives an  $E1$  multipolarity for the 1746.0 keV transition from this state to the  $2_1^+$  state. Also the negative  $A_{22}$  angular-distribution coefficient implies a  $\Delta I = 1$  character for this transition (Table II). The  $(p, 2n)$  excitation-function curve indicates an  $I = 3$  for this state (Fig. 4). Thus, this state can firmly be assigned  $I^\pi = 3^-$ . The state could well be the same one as the proposed  $3^-$  state at 2366 keV of Ref. [35], where the levels separated by less than 50 keV were not resolved.

## B. The nucleus $^{108}\text{Cd}$

Based on the measurements of the present work we have established for the  $^{108}\text{Cd}$  isotope three new levels below the 2.5 MeV excitation energy, four new or revised  $I^\pi$  assignments, and about 10 new transitions. One level previously reported was not confirmed.

The data of Table III and of Fig. 5 are consistent with the earlier assignments [21] of  $4_1^+$  and  $2_2^+$  for the 1508.3 and 1601.7 keV states, respectively.

The 1721.0 keV level is strongly populated in the  $(^3\text{He}, d)$  proton-transfer reaction and suggested to have  $I^\pi = (0-2)^+$  [36]. A level at 1704(25) keV has been observed in the  $(d, ^6\text{Li})$  alpha-transfer reaction [37], which

TABLE II. Properties of levels and transitions in  $^{106}\text{Cd}$  as obtained in this work.

$E_{\text{level}}^a$ (keV)	$J_i^\pi$	$E_{\text{trans}}^a$ (keV)	$J_f^\pi$	$\gamma$ intensity <sup>b</sup>			$10^3 \cdot \alpha_K^d$	Ang. Distr. Coeff.		Multi- polarity
				$(p, p')^c$	$(p, 2n)$	In decay		$A_{22}$	$A_{44}$	
632.6	$2_1^+$	632.6	$0_1^+$	1000	1000	1000	3.0(1) <sup>j</sup>	0.17(1)	-0.06(2)	$E2$
1493.8	$4_1^+$	861.2	$2_1^+$	128	390	313	1.4(1)	0.24(1)	-0.06(2)	$E2$
1716.6	$2_2^+$	1084.0	$2_1^+$	197	43	27	0.84(10)	-0.14(1)	-0.06(2)	$E2/M1$
		1716.6	$0_1^+$	168	47 <sup>e</sup>	154 <sup>f</sup>				
1795.3	$0_2^+$	1162.7	$2_1^+$	164	14	12	0.68(9)	-0.03(2)	-0.10(3)	$E2$
2104.6	$4_2^+$	388.0	$2_2^+$	1.8(4)	2.5	2.3		0.38(5)	-0.23(7)	$E2$
		610.7	$4_1^+$	34	65	28	3.7(4)	0.09(1)	-0.04(2)	$E2/M1$
		1472.0	$2_1^+$	20	37	16	0.37(5)	0.27(1)	-0.06(1)	$E2$
2143.9	$0_3^+$	427.2	$2_2^+$	33	3.9	1.4	8.4(10) <sup>d</sup>	0.14(7)	-0.05(10)	$E2$
		1511.4	$2_1^+$	101	7.3	3.4	0.40(15) <sup>d</sup>	-0.08(6)	-0.03(9)	$E2$
		2143.9	$0_1^+$			<0.1	>42 <sup>g</sup>			$E0$
2252.2(6)	$(4^+)$	758.8	$4_1^+$	9.5	2.3	1.9		0.30(10)	-0.14(14)	$(E2/M1)$
		1619.6(6)	$2_1^+$	190(90)	44	39 <sup>h</sup>	0.34(5) <sup>i</sup>			
2254.0(5)	$(2^+, 3^+)$	536.2	$2_2^+$	6.5	2.2			-0.48(23)	0.01(36)	$(E2/M1)$
		1621.4(4)	$2_1^+$	100(50)	15	h	i			
2305.1	$4^+$	811.2	$4_1^+$	38	28	9.6	1.8(3)	-0.14(7)	0.08(1)	$E2/M1$
		1672.6	$2_1^+$	4.8	3.7	1.9	<0.45	0.34(5)	-0.16(7)	$E2$
2330.5	$5_1^+$	225.9	$4_2^+$	28	31	17	55(6)	-0.77(3)	-0.005(44)	$E2/M1$
		836.8	$4_1^+$	8.3	22	6.5	2.6(4)	-0.37(3)	-0.06(5)	$E2/M1$
2347.3		1714.7	$2_1^+$	185	24(6) <sup>e</sup>	f				
2370.6	$(2)^+$	575.3	$0_2^+$	25	1.8	3.7	3.6(5) <sup>d</sup>			$E2$
		653.9	$2_2^+$	30	2.6	4.6		0.05(5)	-0.12(7)	$E2/M1$
		1738.0	$2_1^+$	90	8.2	12		-0.14(3)	-0.10(4)	$E2/M1$
		2370.6	$0_1^+$	6.3	1.0					
2378.6	$3_1^-$	1746.0	$2_1^+$	121	43	12	<0.15	-0.22(3)	-0.02(5)	$E1$

<sup>a</sup>Energy uncertainties typically 0.3 keV.

<sup>b</sup>Intensity error typically 15%. Intensity of the  $2_1^+ - 0_1^+$  transitions normalized to 1000.

<sup>c</sup>Gamma-ray intensities from the  $(p, p')$  reaction correspond to the direct level population.

<sup>d</sup>The  $K$  internal-conversion coefficients are determined from the In decay experiments except the ones marked with (d) are from the  $(p, p')$  experiments.

<sup>e</sup>Intensity determined from the  $\gamma\gamma$ -coincidence spectra.

<sup>f</sup>Intensity contains the 1716.6 and 1714.7 keV transitions; see the data for the 1716.6 keV transition.

<sup>g</sup> $E0$  transition;  $\alpha_K > 35 \times \alpha_K(M4)$ .

<sup>h</sup>Intensity contains the 1619.6 and 1621.4 keV transitions; see the data for the 1619.6 keV transition.

<sup>i</sup>Conversion coefficient for the sum of the 1619.6 and 1621.4 keV transitions.

<sup>j</sup>Conversion coefficient normalized to  $\alpha_K = 3.0(1)$  for the 632.6 keV line.

could be considered to be the same level. From the proton gated  $\gamma$ -ray spectra we establish a strong 1088.1 keV transition from this state to the  $2_1^+$  state. The  $\gamma\gamma$ -coincidence measurement in the  $(p, 2n)$  reaction confirms the placement. This agrees with the information for the 1087.6 keV  $\gamma$  ray given by Roussiere *et al.* [18], although it was not placed into their level scheme. In our work, both the isotropic angular-distribution and the excitation-function curve (Fig. 5) of the 1088.1 keV gamma-ray determine  $I=0$  for this level. Consequently, the state must be the first excited  $0^+$  state in  $^{108}\text{Cd}$ . As in the case of the  $0_2^+$  state in  $^{106}\text{Cd}$ , no  $E0$  transition from this state to the ground state is observed.

The 1913.3 keV level has previously been assigned as  $I^\pi=0^+$  by Roussiere *et al.* [18] based on the observed  $E0$  transition to the ground state. Our data confirm the assignment. The  $E0$  transition can be seen in Fig. 8, which shows the conversion-electron and  $\gamma$ -ray spectra from the  $^{108}\text{In}$  decay. The  $\gamma$ -ray branching ratio of the 311.3 and 1280.6 keV  $E2$  transitions is consistent with the results of Ref. [18].

The 2020.7 keV level and the depopulating 1387.8 keV transition reported in Ref. [18] are not observed in any of

our experiments. Thus, the level was omitted from the level scheme of  $^{108}\text{Cd}$ .

At 2145.6 keV we find a new level which deexcites to the  $2_1^+$ ,  $4_1^+$ , and  $2_2^+$  levels. These transitions are placed on the basis of the  $\gamma\gamma$ - and  $p\gamma$ -coincidence experiments. From the present conversion coefficient of the 1512.7 keV transitions, positive parity is deduced for this state. On the basis of the negative  $A_{22}$  angular-distribution coefficients for the 544.2 and 1512.7 keV  $\gamma$  rays and the excitation-function curve (Fig. 5) of the 1512.7 keV  $\gamma$  ray, we propose an  $I=3$  for this state, thus suggesting  $I^\pi=(3)^+$ .

The level at 2162.5 keV has earlier been assigned as  $3^-$  [18,38]. From the conversion-electron and  $\gamma$ -ray spectra of Fig. 8, one clearly sees that the 1529.6 keV transition from this state to the  $2_1^+$  state has a multipolarity of  $E2/M1$  rather than  $E1$ . In Ref. [18] the  $E1$  multipolarity is determined for the 1529.7 keV transition based on their experimental  $K$ -conversion coefficient. This value is the only one of those reported in Ref. [18], which is in serious disagreement with our results. Since the transition from this state to the ground state is observed in the present work, a spin and parity  $2^+$  is adopted. The excitation function (Fig. 5) and the angular distribution of the 1529.6 keV  $\gamma$  ray are in agreement with the  $2^+$  assignment.

The 2201.9 keV level is confirmed to have  $I^\pi=3^-$  by the 1569.0 keV  $E1$  transition to the  $2_1^+$  state, which is shown in Fig. 8. Moreover, a new 600.2 keV transition to the  $2_2^+$  level is observed in the present work.

The 2239.2 keV level has previously been assigned as  $4^+$  [18], which agrees with our data.

For the 2365.7 keV level, our experiments have confirmed the  $2^+$  assignment reported in Ref. [38]. The  $\gamma$ -ray branching ratio agrees with Ref. [21].

At 2374.7 keV a new level is located. The level is depopulated by the 1741.8 and 772.7 keV transitions to the  $2_1^+$  and  $2_2^+$  states, respectively. In Ref. [18] an unplaced transition of 1741.8 keV is reported. The  $E2/M1$  multipolarity (Table III and Fig. 8) for both of the transitions indicate positive parity. The angular distribution of the 1741.8 keV transition favors a spin of 0, but the assignment is not conclusive.

The new level at 2486.1 keV might be the 2481 keV level observed in the  $(^3\text{He}, d)$  reaction [36]. We have seen the depopulating transitions of 1853.2 and 884.5 keV to the  $2_1^+$  and  $2_2^+$  states, respectively, and the transition to the ground state. This, together with the excitation-function curve for the 1853.2 keV transition (Fig. 5), reveals  $I^\pi=2^+$  for the state. Also the  $E2/M1$  multipolarity of the 1853.2 keV transition is consistent with the  $2^+$  assignment.

### C. The nucleus $^{110}\text{Cd}$

Our data for  $^{110}\text{Cd}$  agree with the results of Kern *et al.* [7], except the 1809.5 keV level ( $I^\pi=2^+$ ), which we do not observe.

The second excited level at 1473.2 keV has previously been identified as a  $0^+$  state through a  $\gamma$ -ray angular-correlation measurement in the  $^{110}\text{Ag}$  decay [39] and a

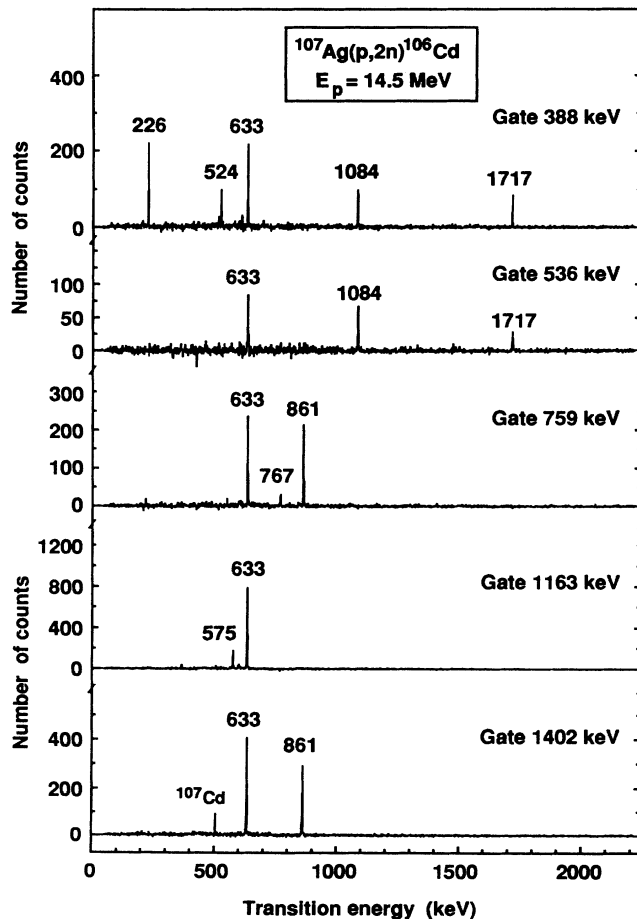


FIG. 14. The  $\gamma\gamma$ -coincidence spectra from the  $^{107}\text{Ag}(p, 2n)$  reaction at  $E_p=14.5$  MeV measured with two NORDBALL-type Compton-suppression spectrometers.

proton-transfer reaction study [36]. The excitation-function curve (Fig. 6) and the angular distribution (Table IV) for the 815.4 keV transition to the  $2_1^+$  state in our  $(\alpha, 2n)$ -reaction experiments are in accordance with this assignment. As in the case of the  $0_2^+$  states in  $^{106}\text{Cd}$  and  $^{108}\text{Cd}$ , we could not observe the  $E0$  transition to the ground state.

Our results for the 1475.9 keV  $2_2^+$  and 1542.5 keV  $4_1^+$  states agree with the previous results for these levels [22,7].

The spin of the 1731.3 keV level was assigned tentatively as  $(0)^+$  based on the  $(^3\text{He}, d)$  data and the level systematics of even Cd isotopes [22]. Our excitation-function (Fig. 6) and angular-distribution (Table IV) measurements for the 1073.7 keV transition to the  $2_1^+$  state in the  $(\alpha, 2n)$  reaction prove that this level has  $I^\pi=0^+$ . Moreover, we have observed a 255.4 keV  $E2$  transition to the  $2_2^+$  state (Fig. 15). The  $E0$  transitions to the  $0_2^+$  state and to the ground state were not observed.

The 1783.6 keV level is known as the third  $2^+$  state [22,7]. Our data agree with this assignment.

We do not observe the 1809.5 keV level seen in the  $^{110}\text{In}$  decay [22] and in the  $(\alpha, 2n)$  reaction [7]. According to our  $\gamma\gamma$ -coincidence measurements in the  $(\alpha, 2n)$  reaction the proposed depopulating 1151.7 keV transition does not belong to the  $^{110}\text{Cd}$  nucleus but most probably to  $^{111}\text{Cd}$  (Fig. 15). Furthermore, there is no evidence for this state in our  $p\gamma$ -coincidence spectra.

The 2078.6 keV level has been assigned as  $I^\pi=0^+$  in the  $^{110}\text{Ag}$  ( $1^+$ ; 24.6 s) decay [39] and in the  $(^3\text{He}, d)$  reaction [36], where it is strongly populated. In our study of the  $^{110}\text{In}$  EC/ $\beta^+$  decay, we have observed new  $E0$  transitions from this state to the ground state and to the 1473 keV  $0_2^+$  state. Our value for the conversion coefficient of the 295 keV transition (Table IV) supports the earlier placement of  $(0_4^+-2_3^+)$ . Other possible  $E2$  transitions from this  $0_4^+$  state are hampered by transitions from the close-lying  $3^-$  state.

TABLE III. Properties of levels and transitions in  $^{108}\text{Cd}$  as obtained in this work.

$E_{\text{level}}^a$ (keV)	$J_i^\pi$	$E_{\text{trans}}^a$ (keV)	$J_f^\pi$	$\gamma$ intensity <sup>b</sup>			Decay	$10^3 \cdot \alpha_K$	Ang. Distr. Coeff.		Multi- polarity
				$(p, p')^c$	$(p, 2n)$				$A_{22}$	$A_{44}$	
632.9	$2_1^+$	632.9	$0_1^+$	1000	1000	1000		3.0(1) <sup>g</sup>	0.18(3)	-0.02(4)	$E2$
1508.3	$4_1^+$	875.4	$2_1^+$	61	343	230		1.4(3)	0.28(4)	-0.03(7)	$E2$
1601.7	$2_2^+$	969.1	$2_1^+$	141	68	46		1.2(2)	-0.09(2)	-0.05(3)	$E2/M1$
		1601.7	$0_1^+$	123	62	47		0.36(5)	0.14(3)	-0.01(5)	$E2$
1721.0	$0_2^+$	1088.1	$2_1^+$	127	15	14		0.8(1)	0.04(2)	-0.04(3)	$E2$
1913.3	$0_3^+$	311.3	$2_2^+$	46	4(1) <sup>d</sup>	7.4		21(3)			$E2$
		1280.6	$2_1^+$	39	5(1)	8.2		0.39(6)	-0.01(17)	-0.01(25)	$E2$
		1913.3	$0_1^+$			< 4		> 25 <sup>e</sup>			
2145.6	$(3)^+$	544.2	$2_2^+$	8.3	6.0	1.5			-0.42(3)	-0.09(5)	$E2/M1$
		637.3	$4_1^+$	f	4(1) <sup>d</sup>	f					
		1512.7	$2_1^+$	62	48	12		0.40(5)	-0.36(2)	-0.00(4)	$E2/M1$
2162.5	$2_3^+$	1529.6	$2_1^+$	80	30	81		0.43(5)	0.12(2)	-0.01(3)	$E2/M1$
		2162.5	$0_1^+$	2.5(10)	1.7	6.2					
2201.9	$3_1^-$	600.2	$2_2^+$	1.8(3)	3.0						
		1569.0	$2_1^+$	54	62	12		0.19(3)	-0.12(3)	-0.01(4)	$E1$
2239.2	$4_2^+$	637.5	$2_2^+$	5.5 <sup>f</sup>	3(1) <sup>d</sup>	6.3 <sup>f</sup>					
		730.9	$4_1^+$	13	27	21		2.9(4)	0.12(4)	-0.03(5)	$E2/M1$
		1606.3	$2_1^+$	8.4	23	17		0.37(5)	0.26(1)	-0.08(2)	$E2$
2365.7	$2_4^+$	1732.8	$2_1^+$	57	17	39		0.32(4)	0.13(4)	0.01(5)	$E2/M1$
		2365.7	$0_1^+$	8.5(25)	2.7	5.3			0.06(6)	-0.16(9)	
2374.7	$(0)^+$	772.7	$2_2^+$	4.6	1.0	5.6		2.3(4)			$(E2)$
		1741.8	$2_1^+$	34	5.4	13		0.32(4)	-0.02(8)	-0.13(11)	$(E2)$
2486.1	$2^+$	884.5	$2_2^+$	3(1)	2.7						
		1853.2	$2_1^+$	34	15	28		0.33(5)	-0.10(2)	-0.00(3)	$E2/M1$
		2486.0	$0_1^+$	1.0(5)							

<sup>a</sup>Energy uncertainties typically 0.3 keV.

<sup>b</sup>Intensity error typically 15%. Intensity of the  $2_1^+-0_1^+$  transitions normalized to 1000.

<sup>c</sup>Gamma-ray intensities from the  $(p, p')$  reaction correspond to the direct level population.

<sup>d</sup>Intensity determined from  $\gamma\gamma$ -coincidence spectra.

<sup>e</sup> $E0$  transition;  $\alpha_K > 17 \times \alpha_K(M4)$ .

<sup>f</sup>Intensity contains the 637.3 and 637.5 keV transitions; see the data for the 637.5 keV transition.

<sup>g</sup>Conversion coefficient normalized to  $\alpha_K = 3.0(1)$  for the 632.9 keV line.

The 2078.9 keV level has been identified in many experiments [22] as a  $3^-$  state. We have observed two depopulating transitions, the 602.9 keV transition to the  $2_3^+$  state and the 1421.2 keV transition to the  $2_1^+$  state. According to our conversion electron data, the latter transition has definitively an  $E1$  character (Table IV) confirming the  $3^-$  assignment.

Our data agree with the earlier assignments of  $3^+$  for the 2162.8 keV level and  $4^+$  for the 2220.2 and 2250.0 keV levels [22,7].

For the levels at 2287.5 and 2332.1 keV, quite strongly populated in our  $(p,p')$  experiments, we are not able to get any definite spin and parity assignments. In the  $(n,n'\gamma)$  study [40] the assignments of  $2^+$  and  $0^+$  were given to these states, respectively.

The level at 2355.8 keV is assigned as  $2^+$  in Ref. [40].

The conversion coefficient of the 1698.0 keV transition feeding the  $2_1^+$  level defines positive parity (Table IV). The excitation-function curve of this transition indicates  $I \geq 4$ , but the angular-distribution coefficient  $A_{22}$  is not consistent with that.

#### D. The nucleus $^{112}\text{Cd}$

We used the  $^{112}\text{Cd}$  nucleus as a reference case for our  $(p,p'\gamma)$  experiments. Especially, we could examine the population of  $0^+$  levels in this reaction. Since no electron spectroscopy is applied in the present work for  $^{112}\text{Cd}$ , the  $E0$  transitions are not included in Table V nor in Fig. 12 summarizing our results. The earlier study of Julin *et al.* [41] is referred for the  $E0$  measurements. The new data from our recently performed  $(\alpha,2n)$  reaction revealed

TABLE IV. Properties of levels and transitions in  $^{110}\text{Cd}$  as obtained in this work.

$E_{\text{level}}^{\text{a}}$ (keV)	$J_i^{\pi}$	$E_{\text{trans}}^{\text{a}}$ (keV)	$J_f^{\pi}$	$(p,p')^{\text{c}}$	$\gamma$ intensity <sup>b</sup> ( $\alpha,2n$ )	Decay	$10^3 \cdot \alpha_K$	Ang. Distr. Coeff. $A_{22}$	$A_{44}$	Multi- polarity
657.8	$2_1^+$	657.8	$0_1^+$	1000	1000	1000	2.7(1) <sup>h</sup>	0.23(2)	-0.15(3)	$E2$
1473.2	$0_2^+$	815.4	$2_1^+$	75	12	2.8	1.6(2) <sup>d</sup>	0.08(12)	-0.08(17)	$E2$
1475.9	$2_2^+$	818.1	$2_1^+$	81	71	9.8	d	-0.23(1)	-0.10(1)	$E2/M1$
		1475.9	$0_1^+$	40	42	5.7	0.46(3)	0.18(3)	-0.11(4)	$E2$
1542.5	$4_1^+$	884.8	$2_1^+$	15	560	50	1.2(2)	0.28(3)	-0.22(5)	$E2$
1731.3	$0_3^+$	255.4	$2_2^+$	2.7	1.0	0.12	23(7)			$E2$
		1073.7	$2_1^+$	20	6.7	1.1	0.85(8)	0.01(6)	-0.07(9)	$E2$
1783.6	$2_3^+$	1125.8	$2_1^+$	33	35	11	0.43(5)	0.21(2)	-0.10(2)	$E2/M1$
		1783.6	$0_1^+$	11	9.7	3.4	0.18(3)	0.18(2)	-0.01(2)	$E2$
2078.6	$0_4^+$	295.3	$2_3^+$	9.2	3.3	0.4	28(5)	-0.06(4)	-0.18(5)	$E2$
		605.4	$0_2^+$			<0.3	>50 <sup>e</sup>			$E0$
		2078.4	$0_1^+$			<0.17	>7 <sup>f</sup>			$E0$
2078.9	$3_1^-$	602.9	$2_2^+$	6.9	5.5	0.7		-0.3(2)	-0.3(3)	$E1$
		1421.2	$2_1^+$	43	39	4.6	0.19(2)	-0.28(3)	-0.04(5)	$E1$
2162.8	$3_1^+$	687.0	$2_2^+$	3.6	8.0	0.7		-0.70(5)	-0.01(2)	$E2/M1$
		1505.0	$2_1^+$	12	25	1.1	0.50(5)	-0.55(4)	-0.03(7)	$E2/M1$
2220.2	$4_2^+$	677.8	$4_1^+$	3.6	26	2.5		0.05(1)	-0.13(2)	$E2/M1$
		744.3	$2_2^+$	1.5	14	1.1	2.0(3)	0.28(1)	-0.27(1)	$E2$
		1562.3	$2_1^+$	<0.7	3.0	0.3		0.22(6)	-0.19(8)	$E2$
2250.5	$4_3^+$	467.0	$2_3^+$		7(3) <sup>g</sup>			0.28(4)	-0.29(5)	$E2$
		708.0	$4_1^+$	2.4	38 <sup>g</sup>			0.45(3)	-0.14(4)	$E2/M1$
		774.7	$2_2^+$		2(1)					
		1592.7	$2_1^+$		5(1)			0.22(3)	-0.16(4)	$E2$
2287.5		1629.7	$2_1^+$	15	10	1.0		0.01(5)	0.01(8)	
2332.1		1674.3	$2_1^+$	12	2.2	0.2		0.14(10)	-0.18(15)	
2355.8		1698.0	$2_1^+$	13	6.9	3.0	0.27(5)	-0.02(1)	-0.12(2)	$E2/M1$

<sup>a</sup>Energy uncertainties typically 0.3 keV.

<sup>b</sup>Intensity error typically 15%. Intensity of the  $2_1^+ - 0_1^+$  transitions normalized to 1000.

<sup>c</sup>Gamma-ray intensities from the  $(p,p')$  reaction correspond to the direct level population.

<sup>d</sup>Conversion coefficient for the sum of the 815.4 and 818.1 keV transitions; see the data for the 815.4 keV transition.

<sup>e</sup> $E0$  transition;  $\alpha_K > 1.6 \times \alpha_K(M4)$ .

<sup>f</sup> $E0$  transitions;  $\alpha_K > 38 \times \alpha_K(M4)$ .

<sup>g</sup>Intensity deduced from  $\gamma\gamma$ -coincidence spectra.

<sup>h</sup>Conversion coefficient normalized to  $\alpha_K = 2.7(1)$  for the 657.8 keV line.

one new level below 2.1 MeV excitation energy and several new transitions. The experimental data for higher-lying levels will be published separately [56].

The results obtained in this work for the four lowest excited levels are consistent with the data given in the  $A=112$  compilation [23]. The  $\gamma$ -ray branching ratio for the transitions from the  $0_3^+$  level obtained in our  $(\alpha, 2n)$  experiment are in disagreement while those obtained from the  $(p, p')$  reaction are in agreement with the results of Ref. [23]. The  $(p, p')$  results have been adopted to the level scheme (Fig. 12), since in the  $(\alpha, 2n)$  case the 815 keV line is a doublet with another 815 keV transition being higher in the level scheme [28,56]. Contrary to the  $(\alpha, 2n)$  study by Geiger *et al.* [28], performed at similar alpha-beam energies as our experiments, we clearly populated the first two excited  $0^+$  levels.

The 1468.8 keV  $2^+$  level has previously been observed to decay to the  $0_2^+, 2_1^+$  and the ground states [23]. Our result is consistent with that. The branching ratios of the depopulating transitions agree with the adopted values [23].

The 1870.8 keV level has been assigned as  $0^+$  in several experiments: via the  $\gamma$ -ray angular-distribution measurements in the photoexcitation study [42], via the  $\gamma$ -ray angular-correlation measurements in the  $^{112}\text{In}$  ( $1^+$ ) decay [39], in the  $^{112}\text{Ag}$  ( $2^-$ ) decay [43], and earlier through particle spectroscopy in the  $(d, p)$  reaction [44]. It has

also been populated in the proton-scattering experiments by Pignanelli *et al.* [45], and recently in the two-neutron  $(t, p)$  transfer reaction [46].

In the earlier  $(\alpha, 2n)$  study Geiger *et al.* [28] report that the first two excited  $0^+$  states are not populated while the 1870 keV  $0^+$  state is. The 402, 558, and 1253 keV transitions to the  $2_3^+, 2_2^+$ , and  $2_1^+$  levels, respectively, have been observed to depopulate this level [28]. In addition to those transitions, we found a new 455 keV transition to the  $4_1^+$  level in our  $\gamma\gamma$ -coincidence measurements from the  $(\alpha, 2n)$  reaction (see the gates 455 and 701 keV in Fig. 16). This result is in serious disagreement with the  $0^+$  assignment for the 1870 keV level. Therefore, we repeated the  $\gamma$ -ray angular-distribution and excitation-function measurements to figure out the spin of the level. The angular distributions of the 402 and 1253 keV transitions are definitely of  $\Delta I=2$  character and not isotropic (Table V) as reported in Ref. [28]. The angular distribution of the 455 keV transition is consistent with  $\Delta I=0$ . The excitation functions indicate spin 4 for the level (Fig. 7). Moreover, the 1870 keV state is fed from the 2570.9 keV level (Fig. 16), which we assign as a  $6^+$  state based on the angular distributions and excitation functions of the depopulating 701 and 1155 keV transitions (Fig. 7, Table V). Thus, we adopt  $I^\pi=4^+$  for the 1870 keV state.

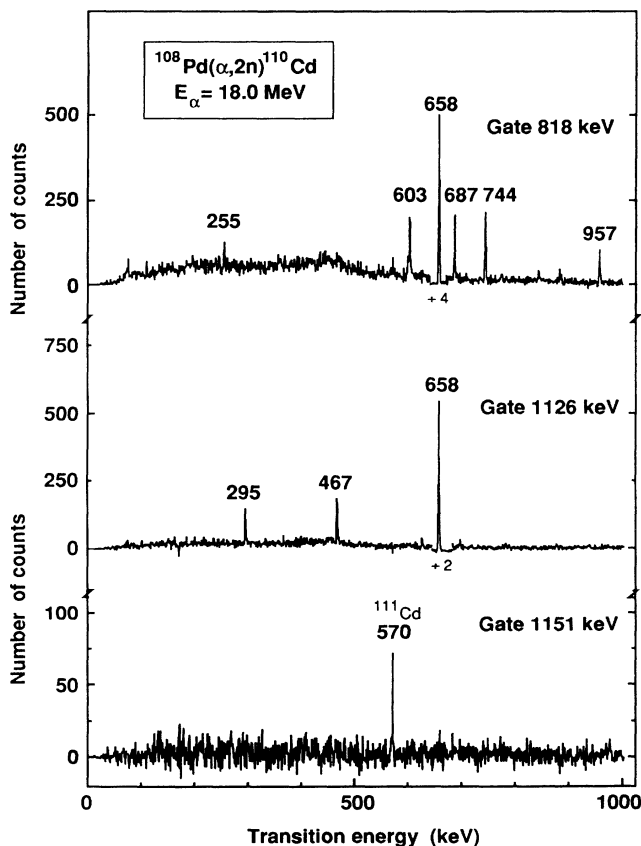


FIG. 15. Gamma-gamma coincidence spectra from the  $^{108}\text{Pd}(\alpha, 2n)^{110}\text{Cd}$  reaction at  $E_\alpha = 18.0$  MeV.

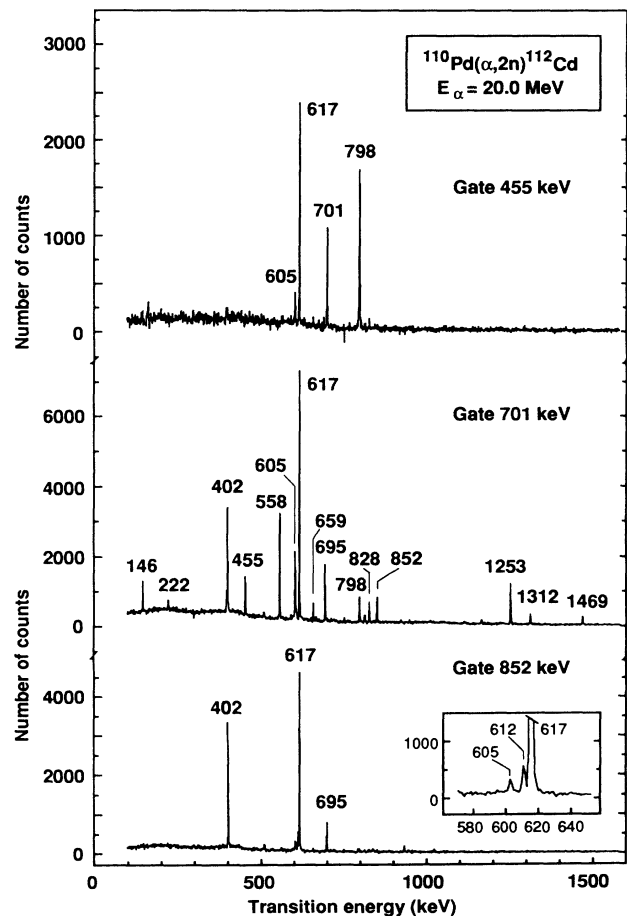


FIG. 16. Gamma-gamma coincidence spectra from the  $^{110}\text{Pd}(\alpha, 2n)^{112}\text{Cd}$  reaction at  $E_\alpha = 20.0$  MeV.

We conclude that there are two levels at about 1870 keV excitation energy: the  $0^+$  and  $4^+$  levels. Very strong evidence for the  $0^+$  level is deduced from the different experiments as stated above. However, the  $4^+$  level is clearly populated in our  $(\alpha, 2n)$  experiment. Most probably in our  $(p, p')$  experiment it is the  $0^+$  level that is populated, since the  $\gamma$ -ray branchings for the depopulating transitions are quite different from those in the  $(\alpha, 2n)$  reaction (Table V). Based on the energies of the transitions to the  $2_1^+$  state observed in the  $(p, p')$  and  $(\alpha, 2n)$  reactions the  $4^+$  state would be 0.6 keV lower in energy than the  $0^+$  state ( $4^+$  at 1870.4 keV and  $0^+$  at 1871.0 keV).

The 2005.1 keV level has previously been assigned as

the first  $3^-$  state. We observed the 692.7 and 1387.6 keV transitions to the  $2_2^+$  and  $2_1^+$  state. In our  $(p, p')$  and  $(\alpha, 2n)$  experiments the intensity of the 692.7 keV transition is higher than reported in Ref. [23]. The excitation-function and angular-distribution results for those transitions are consistent with the  $3^-$  assignment.

Our data for the 2064.1 keV level are in agreement with the assignment of  $3^+$  for the level and the  $\gamma$ -ray branchings are about the same as in Ref. [23].

The 2081.5 keV level has been assigned as  $4^+$  [23]. In addition to the 666.1 keV transition to the  $4_1^+$  level, we observed in the  $(\alpha, 2n)$  reaction three new transitions: the 211.0, 612.8, and 769.3 keV transitions to the  $4_2^+$ ,  $2_3^+$ , and  $2_2^+$  states, respectively (see the 852 keV gate in Fig.

TABLE V. Properties of levels and transitions in  $^{112}\text{Cd}$  as obtained in this work.

$E_{\text{level}}^{\text{a}}$ (keV)	$J_i^{\pi}$	$E_{\text{trans}}^{\text{a}}$ (keV)	$J_f^{\pi}$	$\gamma$ intensity <sup>b</sup>		Ang. Distr. Coeff.		Multi- polarity
				$(p, p')^{\text{c}}$	$(\alpha, 2n)$	$A_{22}$	$A_{44}$	
617.4	$2_1^+$	617.4	$0_1^+$	1000	1000	0.18(2)	-0.09(3)	$E2$
1224.2	$0_2^+$	606.7	$2_1^+$	12	6.3 <sup>d</sup>	-0.02(7) <sup>f</sup>	-0.08(10)	$E2$
1312.3	$2_2^+$	694.8	$2_1^+$	24	92	-0.24(2)	0.00(3)	$E2/M1$
		1312.3	$0_1^+$	7.8	32	0.13(2)	-0.06(3)	$E2$
1415.3	$4_1^+$	797.9	$2_1^+$	17	670	0.24(2)	-0.12(3)	$E2$
1433.2	$0_3^+$	121.0	$2_2^+$	2.5	1.4	0.08(5)	0.10(7)	$E2$
		815.8	$2_1^+$	4.1	5.1 <sup>e</sup>			
1468.8	$2_3^+$	244.8	$0_2^+$	<0.4	1.7 <sup>e</sup>			
		851.2	$2_1^+$	8.0	34	0.16(1)	-0.02(2)	$E2/M1$
		1468.8	$0_1^+$	3.8	19	0.18(2)	-0.06(2)	$E2$
1870.4	$4_2^+$	401.9	$2_3^+$		24	0.21(3)	-0.11(4)	$E2$
		455.1	$4_1^+$		11	0.03(2)	-0.10(3)	$E2/M1$
		558.3	$2_2^+$		32 <sup>e</sup>	0.08(2) <sup>f</sup>	-0.09(3)	$E2$
		1253.0	$2_1^+$		30 <sup>e</sup>	0.21(1) <sup>f</sup>	-0.11(2)	$E2$
1871.0	$0_4^+$	402.0	$2_3^+$	<0.2				
		558.0	$2_2^+$	<0.3				
		1253.6	$2_1^+$	4.9				
2005.1	$3_1^-$	692.7	$2_2^+$	11	15 <sup>d</sup>	-0.06(1) <sup>f</sup>	0.03(2)	$E1$
		1387.7	$2_1^+$	18	33	-0.22(3)	-0.00(5)	$E1$
2064.1	$3_1^+$	649.0	$4_1^+$		7 <sup>e</sup>			
		751.8	$2_2^+$	1.6	21 <sup>e</sup>			
		1446.8	$2_1^+$	1.3	13	-0.51(6)	0.32(9)	$E2/M1$
2081.0	$4_3^+$	211.0	$4_2^+$		1.9 <sup>e</sup>			
		612.8	$2_3^+$		6.4 <sup>e</sup>			
		666.0	$4_1^+$	<0.7	30	0.05(2)	-0.03(4)	$E2/M1$
		769.3	$2_2^+$		23 <sup>e</sup>	0.24(3) <sup>f</sup>	-0.11(4)	$E2$
2570.9 <sup>g</sup>	$6_2^+$	403.8	$6_1^+$		<1.7	0.2(2)	0.1(2)	$E2/M1$
		700.6	$4_2^+$		47	0.25(2)	-0.18(3)	$E2$
		1155.5	$4_1^+$		53	0.02(4)	-0.13(6)	$E2$

<sup>a</sup>Energy uncertainties typically 0.3 keV.

<sup>b</sup>Intensity error typically 15%. Intensity of the  $2_1^+ - 0_1^+$  transitions normalized to 1000.

<sup>c</sup>Gamma-ray intensities from the  $(p, p')$  reaction correspond to the direct level population.

<sup>d</sup>Doublet line: Intensity contains also the higher lying other transition.

<sup>e</sup>Intensity deduced from the  $\gamma\gamma$ -coincidence spectra.

<sup>f</sup>Doublet line: The angular distribution coefficients determined from singles gamma-ray intensities containing both transitions.

<sup>g</sup>Other levels between the 2081 keV level and the 2570.9 keV level omitted; see Ref. [56].



16). The excitation-function and angular-distribution results for those transitions are consistent with the  $4^+$  assignment.

### E. The nucleus $^{116}\text{Cd}$

For  $^{116}\text{Cd}$  we carried out only a short experiment to complete our  $(p,p'\gamma)$  results. The in-beam conversion electron spectra from the  $(p,p')$  reaction were obscured by the dominating  $\beta^-$  background. The beta-decaying  $^{116}\text{In}$  was produced in the  $(p,n)$  reaction. Thus, for this Cd isotope we could not observe any  $E0$  transitions like for the other Cd isotopes. The spin assignments given in Table VI and the level scheme of  $^{116}\text{Cd}$  (Fig. 13) are based on the previous results of Refs. [24] and [47]. Generally, the gamma-ray branchings obtained in this work are in agreement with those of Ref. [24].

The 1282.5 keV level has earlier been assigned tentatively as the first excited  $0^+$  state [24]. We do not observe the 68.9 keV transition to the  $2_2^+$  state as reported from the  $^{116}\text{Ag}$  decay [48,49]. Our upper limit for the  $\gamma$ -ray intensity ratio of the depopulating transitions  $I_\gamma(69\text{ keV})/I_\gamma(769\text{ keV}) < 0.005$  is considerably lower than the value of 0.22 in Ref. [49]. Moreover, the proposed [49] 69 keV transition feeding this  $0_2^+$  level from the 1951 keV  $2^+$  level is not observed in the present work. Instead, the 769 keV  $\gamma$ -ray gated proton spectrum shows a weak population from a level around 2430 keV (this energy region is not included into our table nor the level scheme). In the recent  $(t,p)$  work [47], a new level at 2431(10) keV was found and it was assigned as  $I^\pi=2^+$ . The observed coincidence relations in Ref. [49] would place the 1151.7

keV transition between the 2431 and 1283 keV levels in contradiction to the original placement in Ref. [49].

The 1380.2 keV level has been unambiguously assigned as  $0^+$  [24,47]. In addition to the 866 keV  $0_3^+-2_1^+$  transition we do not observe any new depopulating transitions from this state. While we especially searched for the 167 keV transition to the  $2_2^+$  state, it was not observed; only an upper limit of the  $\gamma$ -ray intensity is determined.

The 1927.8 keV level, strongly populated in our  $(p,p'\gamma)$  experiment, is most probably the  $0_4^+$  state. In a  $(n,n'\gamma)$  study [50], the 1414.3 keV transition has an isotropic angular distribution and, in a  $(t,p)$  study [47], the 1924 keV proton group has a definite  $L=0$  component. In the other  $(n,n'\gamma)$  work [40] the 1929.0(5) keV level has been assigned as a probable  $0^+$  state.

## IV. LEVEL SYSTEMATICS

In Table VII, available ratios of  $E0$  and  $E2$  transition rates [ $X=B(E0)/B(E2)$ ] from  $0_2^+$  and  $0_3^+$  states in the even  $^{106-114}\text{Cd}$  isotopes have been collected. The  $X$  values for  $^{106}\text{Cd}$ ,  $^{108}\text{Cd}$ , and  $^{110}\text{Cd}$  are from the present work. The  $X$  values reported [25] for  $^{110}\text{Cd}$  during the course of this work are in agreement with our values. The  $X$  values for  $^{112}\text{Cd}$  and  $^{114}\text{Cd}$  are from our earlier study [41].

In Table VIII, available level energies and ratios of  $E2$  transition rates relevant to the following discussion have been collected. The values for  $^{106-112}\text{Cd}$  and  $^{116}\text{Cd}$  are from the present work. The values for  $^{114}\text{Cd}$  are from Refs. [51] and [17]. For  $^{118}\text{Cd}$  and  $^{120}\text{Cd}$ , we have used the results of Refs. [15] and [14].

It is now intriguing to examine the systematic behavior of the  $(0_2^+, 2_2^+, 4_1^+, 0_3^+, 2_3^+)$  quintuplet of states (Fig. 17). In  $^{110}\text{Cd}$ ,  $^{112}\text{Cd}$ ,  $^{114}\text{Cd}$ , and  $^{116}\text{Cd}$  these states are well separated from higher-lying states. In  $^{108}\text{Cd}$  (Fig. 10) and  $^{106}\text{Cd}$  (Fig. 9), the  $2_3^+$  state rises fast in excitation energy. In  $^{108}\text{Cd}$  it lies above the 2146 keV  $(3)^+$  state, and in  $^{106}\text{Cd}$ , there are even difficulties in identifying it from the group of the other states. In  $^{106}\text{Cd}$  also the  $0_3^+$  state lies above the  $4_2^+$  state.

In our earlier study [41] we have observed fast  $E2$  transitions from the  $0_2^+$  state to the  $2_1^+$  state of  $^{112}\text{Cd}$  and  $^{114}\text{Cd}$ , 51(13) W.u. and 41(8) W.u., respectively. The small  $X$  values for the  $0_2^+$  states of  $^{106}\text{Cd}$ ,  $^{108}\text{Cd}$ , and  $^{110}\text{Cd}$  also indicate enhanced deexciting  $E2$  transitions. Otherwise the  $B(E0)$  value should be exceptionally small compared to the weakest  $E0$  transitions observed in this mass region. In  $^{116}\text{Cd}$  it is the  $0_3^+$  state which is characterized by a fast  $E2$  transition to the  $2_1^+$  state, as found in the Coulomb-excitation experiment [24], and recently confirmed by Mach *et al.* [16]. The  $B(E2; 0_3^+-2_1^+)$  value deduced from those experiments is about 30 W.u.

On the basis of excitation energies of Refs. [14] and [15] it is now tempting to further speculate if the  $0_3^+$  states in  $^{118}\text{Cd}$  and  $^{120}\text{Cd}$  could be related to the  $0_3^+$  state of  $^{116}\text{Cd}$  and, consequently, to the  $0_2^+$  states of the lighter even isotopes. This kind of conclusion has also been drawn in a recent  $(t,p)$  transfer strength study [13]. Moreover, the relatively short lifetime ( $\tau < 10$  ps) mea-

TABLE VI. Properties of levels and transitions in  $^{116}\text{Cd}$  as obtained in this work.

$E_{\text{level}}^a$ (keV)	$J_i^\pi$	$E_{\text{trans}}^a$ (keV)	$J_f^\pi$	$\gamma$ intensity <sup>b</sup> ( $p,p'$ )
513.5	$2_1^+$	513.5	$0_1^+$	1000
1212.7	$2_2^+$	699.4	$2_1^+$	129
		1212.6	$0_1^+$	75
1219.0	$4_1^+$	705.5	$2_1^+$	4.3
1282.5	$0_2^+$	769.0	$2_1^+$	40
1380.2	$0_3^+$	866.7	$2_1^+$	31
1641.5	$2_3^+$	422.7	$4_1^+$	< 1.3
		1128.5	$2_1^+$	15
		1641.5	$0_1^+$	13
1915.2	$3_1^+$	702.7	$2_2^+$	< 1.3
		1401.8	$2_1^+$	< 2.7
1921.2	$3_1^-$	708.7	$2_2^+$	15
		1407.5	$2_1^+$	50
1927.8	$(0^+)$	1414.3	$2_1^+$	103
1951.0	$2_4^+$	1437.5	$2_1^+$	9

<sup>a</sup>Energy uncertainties typically 0.3 keV.

<sup>b</sup>Intensity error typically 15%. Gamma-ray intensities from the  $(p,p')$  reaction correspond to the direct level population.

TABLE VII. Ratios of  $E0$  and  $E2$  transition rates for  $0_2^+$  and  $0_3^+$  states in the even  $^{106-114}\text{Cd}$  isotopes.

$X_{ijk}^a$	Mass number				
	106	108	110	112 <sup>b</sup>	114 <sup>b</sup>
$X_{211} (10^{-3})$	<9	<12	<8	26(4)	26(5)
$X_{311}$	2.2(5)	10(2)	<0.04	1.0(2)	16(3)
$X_{312} (10^{-4})$	70(20)	80(20)	<6	2.6(6)	6.0(6)

$$^a X_{ijk} = B(E0; 0_i^+ - 0_j^+) / B(E2; 0_i^+ - 2_k^+).$$

<sup>b</sup>From Ref. [41].

sured by Mach *et al.* [16] for the  $0_3^+$  state in  $^{118}\text{Cd}$  indicating a fast  $0_3^+ - 2_1^+$  transition supports this interpretation.

A characteristic feature of the  $0_3^+$  states in the even  $^{106-114}\text{Cd}$  isotopes is the large value for the ratio  $R = B(E2; 0_3^+ - 2_2^+) / B(E2; 0_3^+ - 2_1^+)$ . In  $^{112}\text{Cd}$  and  $^{114}\text{Cd}$  we have shown this to be due to the hindered  $E2(0_3^+ - 2_1^+)$  transitions, having  $B(E2)$  values of 0.017(4) and 0.0038(5) W.u., respectively [41]. The large  $X_{311}$  values in  $^{106}\text{Cd}$  and  $^{108}\text{Cd}$  (Table VII) reveal that this is also the case in these nuclei.

In  $^{110}\text{Cd}$ , i.e., at  $N=62$ , a discontinuity in the properties of the  $0_3^+$  states is observed. In addition to the small bump in the level-energy curve at  $N=62$ , the smooth decrease of the  $R$  value with decreasing neutron number is disturbed by the smaller value of  $R = 170$  in  $^{110}\text{Cd}$  (Table VIII). Also the limit for the  $X_{311}$  value (Table VII) in  $^{110}\text{Cd}$  is exceptionally low.

From the conclusion that the  $0_3^+$  states in  $^{116}\text{Cd}$ ,  $^{118}\text{Cd}$ , and  $^{120}\text{Cd}$  could be related to the  $0_2^+$  states of the even  $^{106-114}\text{Cd}$  isotopes follows that the  $0_2^+$  states of the  $^{116-120}\text{Cd}$  might be associated with the  $0_3^+$  states of the

TABLE VIII. Relative  $E2$  transition rates in the even  $^{106-120}\text{Cd}$  isotopes. The errors estimated to be between 15% and 35% are not marked.

	106	108	110	112	114 <sup>a</sup>	116	118 <sup>b</sup>	120 <sup>c</sup>
$E(2_2^+)$ (keV)	1716.6	1601.7	1475.9	1312.3	1209.7	1212.7	1269.5	1322.8
$B(E2; 2_2^+ - 2_1^+)$	4 <sup>d</sup>	8 <sup>d</sup>	24 <sup>d</sup>	26 <sup>d</sup>	45 <sup>d</sup>	19 <sup>d</sup>	17	25
$B(E2; 2_2^+ - 0_1^+)$	1	1	1	1	1	1	1	1
$E(0_2^+)$ (keV)	1795.3	1721.0	1473.2	1224.2	1134.5	1282.5	1285.8	1388.7
$B(E2; 0_2^+ - 2_2^+)$	<700	<190	h	h	h	<870		
$B(E2; 0_2^+ - 2_1^+)$	1	1				1		
$E(0_3^+)$ (keV)	2143.9	1913.3	1731.3	1433.2	1305.6	1380.2	1615.0	1744.6
$B(E2; 0_3^+ - 2_2^+)$	230	1100	170	8500	41000	<240	<19	<3
$B(E2; 0_3^+ - 2_1^+)$	1	1	1	1	1	1	1	1
$E(2_3^+)$ (keV)	2370.6	2162.5	1783.6	1468.8	1364.3	1641.5	1915.8	2093.8
$B(E2; 2_3^+ - 0_1^+)$	1	1	1	1	1	1		1
$B(E2; 2_3^+ - 2_1^+)$	50	<100	<33	<28	<50	<10	<10 <sup>f</sup>	<33
$B(E2; 2_3^+ - 2_1^+)^g$			0.5 <sup>d</sup>	0.7 <sup>d</sup>	0.2 <sup>d</sup>	2.6 <sup>e</sup>		
$B(E2; 2_3^+ - 4_1^+)$	<1.5	<70	<1100		40	<120	<20	190
$B(E2; 2_3^+ - 2_2^+)$	<2250	<300	<130	<2400	95	<70	330	<700
$B(E2; 2_3^+ - 0_2^+)$	3400	<300	<130	710	50	<140	<30	
$B(E2; 2_3^+ - 0_3^+)$	<4000	<3500			20	<500		

<sup>a</sup>Data from Ref. [17].

<sup>b</sup>Data from Ref. [15].

<sup>c</sup>Data from Ref. [14].

<sup>d</sup> $E2/M1$  mixing ratio from Ref. [55].

<sup>e</sup> $E2/M1$  mixing ratio  $\delta = -0.6$  used from Ref. [50].

<sup>f</sup> $B(E2)$  value normalized to 10.

<sup>g</sup> $B(E2; 2_3^+ - 2_1^+)$  when the  $E2/M1$  mixing ratio used.

<sup>h</sup>Transitions energetically not possible.

lighter even-mass isotopes. Unfortunately, it is difficult to determine the ratio  $R$  in the even  $^{116-120}\text{Cd}$  since it is hard to observe the low-energy  $E2(0_2^+ - 2_2^+)$  transitions. From the data of Ref. [49] an  $R$  value of about  $40 \times 10^3$  is obtained for the  $0_2^+$  state in  $^{116}\text{Cd}$ , while our measurement gave an upper limit of  $R < 870$  (Table VIII). However, noncollectivity of the  $E2(0_2^+ - 2_1^+)$  transition was revealed in the lifetime measurement by Mach *et al.* [16], which leads to a  $B(E2; 0_2^+ - 2_1^+)$  value of 0.95(6) W.u. in  $^{116}\text{Cd}$ .

Arguments for connecting the  $0_2^+$  states in  $^{118}\text{Cd}$  and  $^{120}\text{Cd}$  are more speculative. In addition to the level-energy systematics more support is given by the lifetime-results of Mach *et al.* [16] indicating some noncollectivity of the  $0_2^+ - 2_1^+$  transition in  $^{118}\text{Cd}$ . Also the  $(t, p)$ -transfer cross sections of Ref. [13] support the idea of associating the  $0_2^+$  state of  $^{118}\text{Cd}$  with the  $0_2^+$  state of  $^{116}\text{Cd}$  and further with the  $0_3^+$  states of  $^{112}\text{Cd}$  and  $^{114}\text{Cd}$ .

As a summary for the level-energy systematics of the two lowest excited  $0^+$  states we conclude that the  $0_2^+$  and  $0_3^+$  states of even Cd isotopes exchange their properties when going over the  $N = 66$  isotope  $^{114}\text{Cd}$ . However, according to our data, no corresponding crossing occurs on the neutron-deficient side, contrary to the suggestion of Ref. [13].

In Fig. 17 and the discussion below we use the notation  $0_A^+$  for the  $0_2^+$  state in  $^{106-114}\text{Cd}$  and the  $0_3^+$  in  $^{116-120}\text{Cd}$ . The  $0_3^+$  states in  $^{106-114}\text{Cd}$  and the  $0_2^+$  states in  $^{116-120}\text{Cd}$  are labeled  $0_B^+$ .

In  $^{106}\text{Cd}$  in 2370.6 keV  $(2)^+$  state is adopted as the  $2_3^+$  state, while the lower-lying  $(2^+, 3^+)$  state could be the first excited  $3^+$  state. Concerning the level energies (Fig. 17) a conspicuous feature is the relationship between the  $2_3^+$  and the  $0_A^+$  states. The ratio of their excitation energies is almost constant [Fig. 17(c)].

## V. DISCUSSION

In the simple quadrupole vibrator model, the  $0_A^+$ ,  $2_2^+$ , and  $4_1^+$  states in the even  $^{106-114}\text{Cd}$  isotopes form a two-phonon triplet. The observed strong  $E2$  branches from these states to the  $2_1^+$  state are in agreement with this interpretation. The  $0_B^+$  and  $2_3^+$  states could then play the role of the three-phonon states which in  $^{112}\text{Cd}$  and  $^{114}\text{Cd}$  are pushed down to form the quintuplet of states. Recently, Fahlander *et al.* [17] have shown that all of the measured  $B(E2)$  values in  $^{114}\text{Cd}$  are in qualitative agreement with the simple vibrator values. The application of the vibrator picture to the heavier even Cd isotopes would lead to the conclusion that the three-phonon  $0^+$

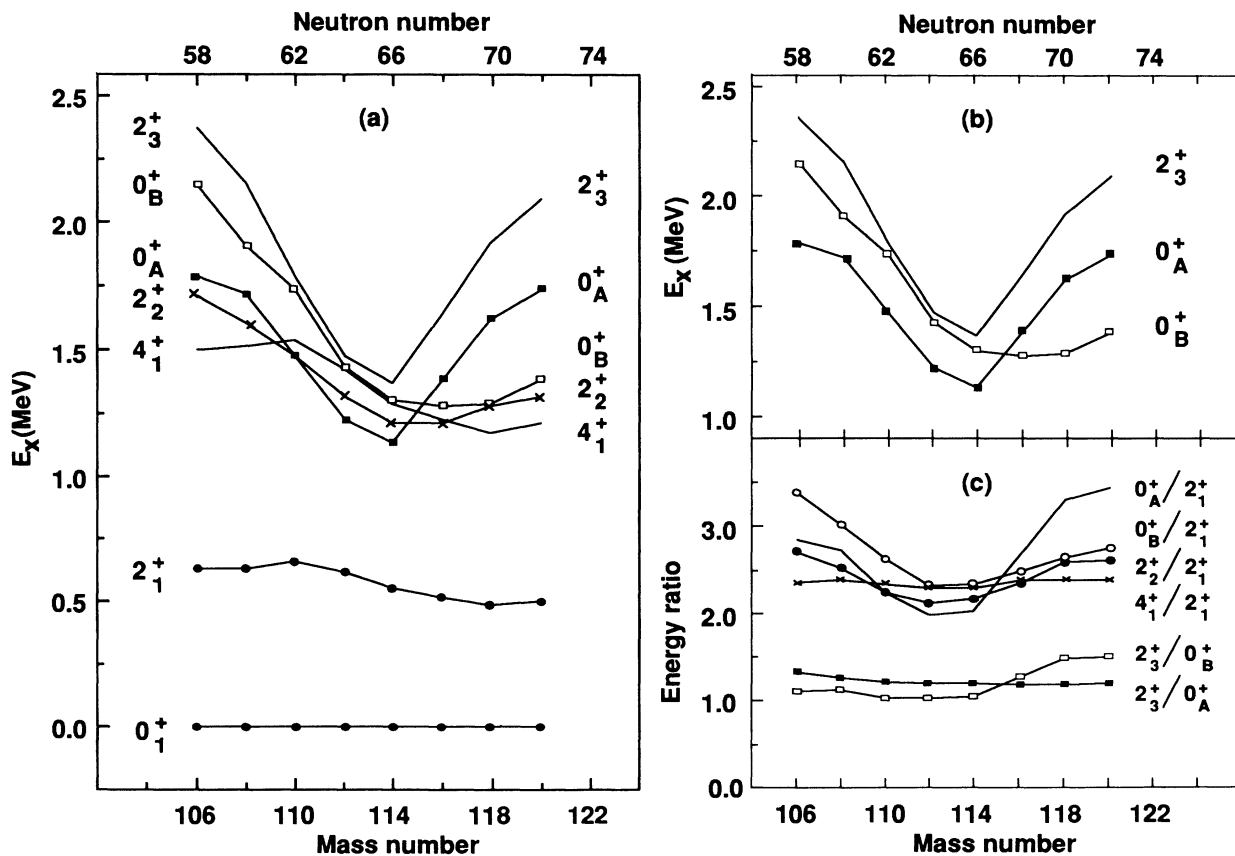


FIG. 17. (a) Systematics of low-lying, low-spin states in the even  $^{106-120}\text{Cd}$ . For clarity of presentation symbols marking the  $2_3^+$  and  $4_1^+$  levels are omitted. (b) Systematics of the  $2_3^+$ ,  $0_A^+$ , and  $0_B^+$  states in the even  $^{106-120}\text{Cd}$ . (c) Energy ratios of the selected levels in even  $^{106-120}\text{Cd}$ .

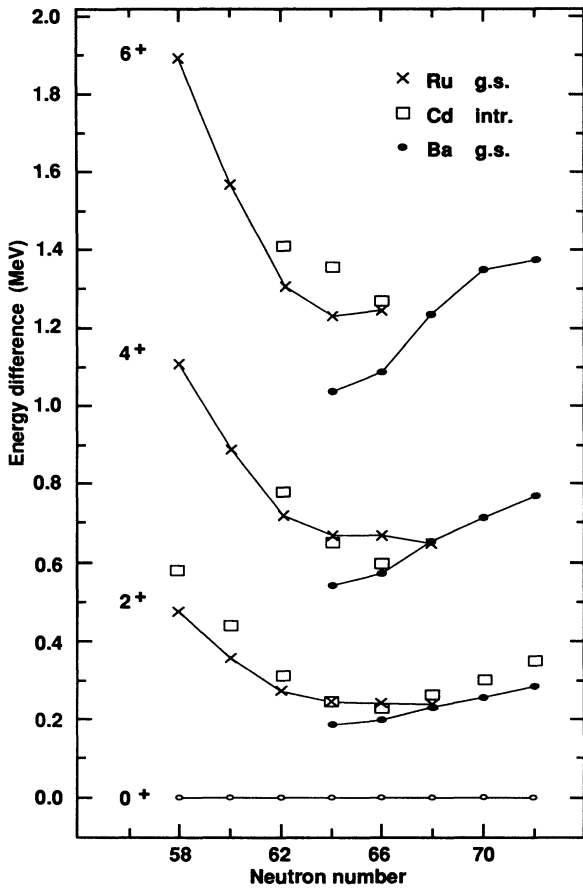


FIG. 18. Proposed members of the intruder band in even  $^{106-120}\text{Cd}$  compared to the members of the ground-state band in the even Ru and Ba isotones. The intruder  $0^+$  state ( $0_A^+$ ) in Cd isotopes is normalized to 0 MeV.

state lies lower than the two-phonon  $0^+$  state. In  $^{134}\text{Ba}$  and  $^{126}\text{Te}$  this kind of phenomenon is explained as caused by  $\gamma$  softness of the nucleus [52,53].

It is intriguing to see if our level systematics exhibit properties characteristic of the behavior of intruder states. The intruder states in the even Cd isotopes should involve proton two-particle-four-hole (2p-4h) excitations, i.e., six valence quasiprotons. The total neutron-proton interaction in these states should be similar to that in the ground-state band of the Ru ( $Z=50-6$ ) and Ba ( $Z=50+6$ ) isotones. In Fig. 18 the members of the band based on the  $0_A^+$  state in the even Cd isotopes are compared with the members of the ground-state band in the corresponding Ru and Ba isotones. The  $2_3^+-0_A^+$  energy difference in the even Cd isotopes is remarkably similar to the  $2_1^+$  energy in the Ru and Ba isotones indicating that the  $0_A^+$  and  $2_3^+$  states could represent the two lowest members of the intruder band. In accordance with the intruder picture, the  $0_A^+$  state has its minimum excitation energy at  $N=66$ , i.e., in the middle of the neutron shell. Also, the analogy between the other band members in  $^{110,112,114}\text{Cd}$  and Ru and Ba isotones is quite impressive (Fig. 18). The continuation of the band above the  $6^+$  state in  $^{110}\text{Cd}$  is not yet clear. The  $8^+$  state of the band reported by Kusnezov *et al.* [10] and Kern *et al.* [7] is not observed in our work, nor in a NORDBALL study [54]. The data for  $^{114}\text{Cd}$  are taken from Refs. [41,51,17]. Our ( $\alpha, 2n$ ) measurements revealed completely new data for  $^{112}\text{Cd}$ .

Further support for associating the  $0_A^+$  states with the intruders comes from a close examination of the results of the two-proton transfer studies where it is clearly the  $0_A^+$  state (and not the  $0_B^+$  state) in  $^{110}\text{Cd}$  and  $^{112}\text{Cd}$  which is populated in the ( $^3\text{He}, n$ ) reaction [5]. It is not obvious

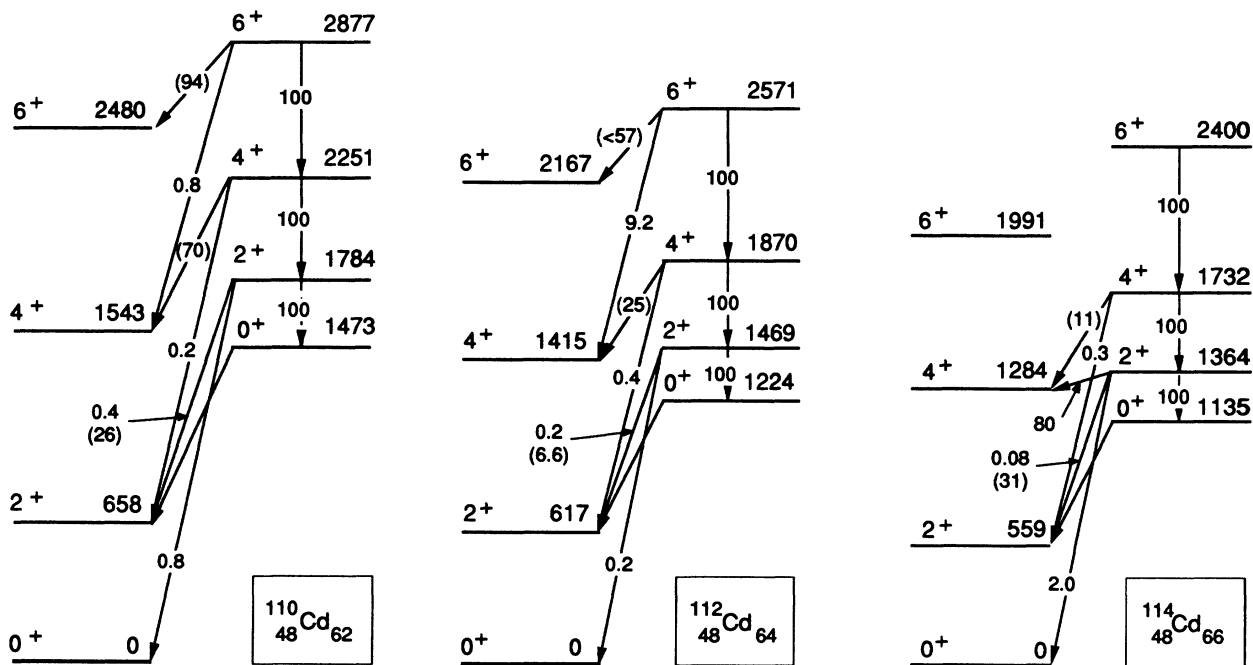


FIG. 19. The intruder band and the ground-state band up to spin  $6^+$  in even  $^{110,112,114}\text{Cd}$ . The relative  $B(E2)$  branching ratios between these bands are marked. In parentheses is given the  $B(E2)$  value when the  $E2/M1$  mixing ratio is not used.

why no  $0^+$  states are strongly populated in  $^{106,108}\text{Cd}$  in the  $(^3\text{He},n)$  reaction. In the evaluation of the  $(t,p)$  transfer strengths, O'Donnell *et al.* [13] have concluded that the  $0^+_A$  state in the even  $^{112-118}\text{Cd}$  isotopes is the intruder.

As mentioned above, in  $^{110}\text{Cd}$ ,  $^{112}\text{Cd}$ , and  $^{114}\text{Cd}$  there are candidates for higher-spin members of the intruder band on top of the  $0^+_A$  state. The ground-state band and the intruder band in these Cd isotopes are shown in Fig. 19. The relative  $B(E2)$  ratios between the ground-state band and the intruder band are from the present work for  $^{110,112}\text{Cd}$  and from Ref. [17] for  $^{114}\text{Cd}$ . The intruder band is clearly rotational.

Many of the  $E2$  and  $E0$  decay properties of even Cd nuclei have been reproduced by introducing a strong mixing of the vibrational and intruder states [10–12]. On the other hand, the similarities in Fig. 18 indicate that the  $2^+_3-0^+_A$  energy differences in the Cd isotopes are not much affected by the mixing. Also the selective population in the  $(^3\text{He},n)$  [5] and  $(t,p)$  [13] reactions do not support the idea of strong mixing. However, weak mixing between the  $0^+$  states would mean that the  $0^+_A$  state plays the role of both a phonon and an intruder state. In Ref. [12] the intruder  $0^+$  state has been associated with the  $0^+$  state having a large  $R$  value, i.e.,  $0^+_B$  state in our notation.

This interpretation is different from ours.

In summary, considerable amounts of new data for the low-lying, low-spin collective states in  $^{106}\text{Cd}$ ,  $^{108}\text{Cd}$ ,  $^{110}\text{Cd}$ , and  $^{112}\text{Cd}$  were obtained in this work by employing various methods of in-beam and off-beam  $\gamma$ -ray and conversion-electron spectroscopy. From the deduced level systematics for the even  $^{106-120}\text{Cd}$  isotopes it is inferred that the excited  $0^+$  states cross between  $^{114}\text{Cd}$  and  $^{116}\text{Cd}$ , i.e., the  $0^+$  states exchange their properties. No corresponding crossing in the neutron deficient isotopes was observed. The second excited  $2^+$  state is found to be closely related to one of the excited  $0^+$  states. In  $^{110}\text{Cd}$ ,  $^{112}\text{Cd}$ , and  $^{114}\text{Cd}$  there were also found higher-spin members of the band built on top of this  $0^+$  state. Interpretation of the results within the mixed intruder and phonon picture has been found to be contradictory.

#### ACKNOWLEDGMENTS

The authors gratefully acknowledge the financial support from the Emil Aaltonen Foundation (J.Ku.) and from the Research Council for Natural Sciences of the Academy of Finland (R.J. and J.Ka.). One of the authors (D.C.) is indebted to the Finnish Ministry for Industry and Trade for financial support.

- 
- [1] K. Heyde, P. Van Isacker, M. Waroquier, J. L. Wood, and R. A. Meyer, *Phys. Rep.* **102**, 291 (1983).
- [2] W. Dietrich, A. Bäcklin, C. O. Lannergård, and I. Ragnarsson, *Nucl. Phys.* **A253**, 429 (1975).
- [3] R. E. Shroy, A. K. Gaigalas, G. Schatz, and D. B. Fossan, *Phys. Rev. C* **19**, 1324 (1979).
- [4] J. Bron, W. H. A. Hesselink, A. Van Poelgeest, J. J. A. Zalmstra, M. J. Uitzinger, H. Verheul, K. Heyde, M. Waroquier, H. Vincx, and P. Van Isacker, *Nucl. Phys.* **A318**, 335 (1979).
- [5] H. W. Fielding, R. E. Anderson, C. D. Zafiratos, D. A. Lind, F. E. Cecil, H. H. Wieman, and W. P. Alford, *Nucl. Phys.* **A281**, 389 (1977).
- [6] R. A. Meyer and L. Peker, *Z. Phys. A* **283**, 379 (1977).
- [7] J. Kern, A. Bruder, S. Drissi, V. A. Ionescu, and D. Kusnezov, *Nucl. Phys.* **A512**, 1 (1990).
- [8] J. Kantele, R. Julin, M. Luontama, A. Passoja, T. Poikolainen, A. Bäcklin, and N.-G. Jonsson, *Z. Phys. A* **289**, 157 (1979).
- [9] A. Bäcklin, N. G. Jonsson, R. Julin, J. Kantele, M. Luontama, A. Passoja, and T. Poikolainen, *Nucl. Phys.* **A351**, 490 (1981).
- [10] D. Kusnezov, A. Bruder, V. Ionescu, J. Kern, M. Rast, K. Heyde, P. Van Isacker, J. Moreau, M. Waroquier, and R. A. Meyer, *Helv. Phys. Acta* **60**, 456 (1987).
- [11] K. Heyde, P. Van Isacker, M. Waroquier, G. Wenes, and M. Sambataro, *Phys. Rev. C* **25**, 3160 (1982).
- [12] A. Aprahamian, D. S. Brenner, R. F. Casten, R. L. Gill, A. Piotrowski, and K. Heyde, *Phys. Lett.* **140B**, 22 (1984).
- [13] J. M. O'Donnell, A. Kotwal, and H. T. Fortune, *Phys. Rev. C* **38**, 2047 (1988).
- [14] A. Aprahamian, Ph.D. thesis, Clark University, 1985; ACS Symposium Series 324, *Nuclei Off the Line of Stability*, edited by R. A. Meyer and D. S. Brenner (American Chemical Society, Washington, DC, 1986), p. 214.
- [15] A. Aprahamian, D. S. Brenner, R. F. Casten, R. L. Gill, and A. Piotrowski, *Phys. Rev. Lett.* **59**, 535 (1987).
- [16] H. Mach, M. Moszynski, R. F. Casten, R. L. Gill, D. S. Brenner, J. A. Winger, W. Krips, C. Wesselborg, M. Büscher, F. K. Wahn, A. Aprahamian, D. Alburger, A. Gelberg, and A. Piotrowski, *Phys. Rev. Lett.* **63**, 143 (1989).
- [17] C. Fahlander, A. Bäcklin, L. Hasselgren, A. Kavka, V. Mittal, L. E. Svensson, B. Varnestig, D. Cline, B. Kotlinski, H. Grein, E. Grosse, R. Kulesa, C. Michel, W. Spreng, H. J. Wollersheim, and J. Stachel, *Nucl. Phys.* **A485**, 327 (1988).
- [18] B. Roussiere, P. Kilcher, J. Sauvage-Letessier, C. Bourgeois, R. Beraud, R. Duffait, M. Meyer, J. Genevey-Rivier, and J. Treherne, *Nucl. Phys.* **A419**, 61 (1984).
- [19] J. Kumpulainen, R. Julin, J. Kantele, A. Passoja, W. H. Trzaska, E. Verho, and J. Väärämäki, *Z. Phys. A* **335**, 109 (1990).
- [20] D. De Frenne, E. Jacobs, M. Verboven, and G. De Smet, *Nucl. Data Sheets* **53**, 73 (1988).
- [21] R. L. Haese, F. E. Bertrand, B. Harmatz, and M. J. Martin, *Nucl. Data Sheets* **37**, 289 (1982).
- [22] P. De Gelder, E. Jacobs, and D. De Frenne, *Nucl. Data Sheets* **38**, 545 (1983).
- [23] D. De Frenne, E. Jacobs, and M. Verboven, *Nucl. Data Sheets* **57**, 443 (1989).
- [24] J. Blachot, J. P. Husson, J. Oms, G. Marguier, and F. Haas, *Nucl. Data Sheets* **32**, 287 (1981).
- [25] A. Giannatiempo, A. Nannini, A. Perego, and P. Sona, *Phys. Rev. C* **41**, 1167 (1990).
- [26] J. Daniere, R. Beraud, M. Meyer, R. Rougny, J.

- Genevey-Rivier, and J. Treherne, *Z. Phys. A* **280**, 363 (1977).
- [27] W. Andrejtscheff, L. K. Kostov, H. Rotter, H. Prade, F. Stary, M. Senba, N. Tsoupas, Z. Z. Ding, and P. Raghavan, *Nucl. Phys. A* **437**, 167 (1985).
- [28] R. Geiger, P. von Brentano, H. G. Friederichs, B. Heits, W. Schuh, K. O. Zell, H. Weigmann, and A. Berinde, *Z. Phys.* **271**, 129 (1974).
- [29] R. Julin, J. Kantele, J. Kumpulainen, M. Luontama, V. Nieminen, A. Passoja, W. Trzaska, and E. Verho, *Nucl. Instrum Methods A* **270**, 74 (1988).
- [30] S. Flanagan, R. Chapman, J. L. Durell, W. Gelletly, and J. N. Mo, *J. Phys. G* **2**, 589 (1976).
- [31] H. Huang, B. P. Pathak, and J. K. P. Lee, *Can. J. Phys.* **56**, 936 (1978).
- [32] R. H. Spear, J. P. Warner, A. M. Baxter, M. T. Esat, M. P. Fewell, S. Hinds, A. M. R. Joye, and D. C. Kean, *Aust. J. Phys.* **30**, 133 (1977).
- [33] B. Roussiere, P. Kilcher, J. Sauvage-Letessier, R. Beraud, R. Duffait, M. Meyer, J. Genevey-Rivier, and J. Treherne, *Proceedings of the Fourth International Conference on Nuclei Far From Stability*, CERN Report 81-09, p. 465.
- [34] L. E. Samuelson, J. A. Grau, S. I. Popik, F. A. Rickey, and P. C. Simms, *Phys. Rev. C* **19**, 73 (1979).
- [35] H. F. Lutz, W. Bartolini, and T. H. Curtis, *Phys. Rev.* **178**, 1911 (1969).
- [36] R. L. Auble, D. J. Horen, F. E. Bertrand, and J. B. Ball, *Phys. Rev. C* **6**, 2223 (1972).
- [37] J. Jänecke, F. D. Becchetti, and C. E. Thorn, *Nucl. Phys. A* **325**, 337 (1979).
- [38] A. I. Muminov, A. Akbarov, B. Ibragimov, D. I. Kochevov, I. K. Kuldzhanov, and R. Razhabbaev, *Izv. Akad. Nauk. SSSR, Ser. Fiz.* **49**, 900 (1985) [*Bull. Acad. Sci. USSR, Phys. Ser.* **49**, No. 5, 60 (1985)].
- [39] Y. Kawase, K. Okano, S. Uehara, and T. Hayashii, *Nucl. Phys. A* **193**, 204 (1972).
- [40] A. M. Demidov, L. I. Govor, Yu. K. Cherepantsev, M. R. Ahmed, S. Al-Najjar, M. A. Al-Amili, N. Al-Assafi, and N. Rammo, *ATLAS of gamma-ray spectra from the inelastic scattering of reactor fast neutrons* (Moscow Atomizdat, Moscow, 1978).
- [41] R. Julin, J. Kantele, M. Luontama, A. Passoja, T. Poikolainen, A. Bäcklin, and N.-G. Jonsson, *Z. Phys. A* **296**, 315 (1980).
- [42] R. Moreh and A. Nof, *Phys. Rev. C* **4**, 2265 (1971).
- [43] G. Wallace, G. J. McCallum, and N. G. Chapman, *Nucl. Phys. A* **182**, 417 (1972).
- [44] P. D. Barnes, J. R. Comfort, and C. K. Bockelman, *Phys. Rev.* **155**, 1319 (1967).
- [45] M. Pignanelli, S. Micheletti, E. Cereda, M. N. Harakeh, S. Y. van der Werf, and R. De Leo, *Phys. Rev. C* **29**, 434 (1984).
- [46] L. R. Medsker, H. T. Fortune, J. D. Zumbro, C. P. Browne, and J. F. Mateja, *Phys. Rev. C* **36**, 1785 (1987).
- [47] D. L. Watson, J. M. O'Donnell, and H. T. Fortune, *J. Phys. G* **13**, 1443 (1987).
- [48] W. B. Walters, in *Proceedings of the International Symposium on Nuclear Orientation and Nuclei Far From Stability*, edited by B. I. Deutch and L. Vanneste [*Hyperfine Interact.* **22**, 317 (1985)].
- [49] W. Bröchle and G. Herrman, *Radiochimica Acta* **30**, 1 (1982).
- [50] T. M. Newton, J. M. Davidson, W. K. Dawson, P. W. Green, H. R. Hooper, W. J. McDonald, G. C. Neilson, and D. M. Sheppard, *Can. J. Phys.* **58**, 8 (1980).
- [51] A. Mheemeeed, K. Schreckenbach, G. Barreau, H. R. Faust, H. G. Börner, R. Brissot, P. Hungerford, H. H. Schmidt, H. J. Scheerer, T. von Egidy, K. Heyde, J. L. Wood, P. Van Isacker, M. Waroquier, G. Wenes, and M. L. Stelts, *Nucl. Phys. A* **412**, 113 (1984).
- [52] R. A. Meyer, R. D. Griffioen, J. Graber Lefler, and W. B. Walters, *Phys. Rev. C* **14**, 2024 (1976).
- [53] S. V. Jackson and R. A. Meyer, *Phys. Rev. C* **15**, 1806 (1977).
- [54] S. Juutinen, R. Julin, P. Ahonen, C. Fahlander, J. Hattula, J. Kumpulainen, A. Lampinen, T. Lönnroth, D. Müller, J. Nyberg, A. Pakkanen, M. Piiparinen, I. Thorslund, S. Törmänen, and A. Virtanen, *Z. Phys. A* **336**, 475 (1990).
- [55] J. Lange, K. Kumar, and J. H. Hamilton, *Rev. Mod. Phys.* **54**, 119 (1982).
- [56] J. Kumpulainen *et al.* (unpublished).